Quantification of the effect of modeled lightning NO_2 on UV-visible air mass factors

Response to Anonymous Referee #1

Joshua L. Laughner and Ronald C. Cohen

October 4, 2017

We thank the reviewer for their positive comments. The individual corrections suggested are addressed below. The reviewer's comments will be shown in red, our response in blue, and changes made to the paper are shown in black block quotes. Unless otherwise indicated, page and line numbers correspond to the original paper. Figures, tables, or equations referenced as "Rn" are numbered within this response; if these are used in the changes to the paper, they will be replaced with the proper number in the final paper. Figures, tables, and equations numbered normally refer to the numbers in the original discussion paper.

1) I think adding a reference to Travis et al., ACP, 2016 (https://www.atmos-chem-phys.net/16/13561/2016/) somewhere in the introduction is important. That paper also called specific attention to the importance of upper troposphere NO2 from lightning, noting that, if ignored, it can lead to underestimates of the air mass factor particularly over the Southeast US. This seems relevant to the manuscript here, and the present authors are listed as co-authors.

We have added a reference to Travis et al. (2016) on p. 2, l. 26.

2) In Section 2.2, could the authors include a statement about the vertical resolution with which WRF was run?

We have added:

> "across a domain that covers the same region as the DC3 campaign at 12 km model resolution **with 29 vertical levels**."

3) In Section 2.5.1, the authors note they have used slant column densities from the NASA Standard Product version 2 (SP v2). Krotkov et al. (2017) recently published documentation for the latest NASA release (SP v3), which includes a new spectral fitting algorithm, and higher resolution profiles. Of course, I dont anticipate the major conclusions of this paper to change. But could the authors include a short statement/argument to reassure the audience this is expected to be the case?

We have added the following text to the second paragraph in Sect. 2.5.1:

> "Version 3 of the NASA Standard Product was released in 2016, and includes new spectral fitting and tropospheric AMF calculations. The change from SP v2

to v3 does not affect any of the AMF calculations in this work. Krotkov et al. (2017) indicates that the tropospheric VCDs over unpolluted areas are similar between SP v2 and v3, therefore, when effects on retrieved VCDs are considered here, we expect our conclusions to be unaltered when BEHR is updated to use SP v3 data."

4) Also in Section 2.5.1, the authors note the use of TOMRAD look-up tables for the pressure-dependent scattering weights. Can anyone access this look-up table data, or is this provided by request from Bucsela et al. specifically for the BEHR retrieval? If the former, could the authors include the location of where this open data could be accessed by others for their own work?

We have added the LUT to the analysis code respository, and mentioned this in the Code and Data Availability section.

5) I am curious whether the default BEHR NO2 retrieval, which uses WRF-Chem model profiles, currently accounts for lightning. I understand this is not directly relevant to the present study (since new a-priori profiles are tested in this case), but it might be useful to point out to the readers, given the authors acknowledge that WRF-Chem is often run by default without lightning NO2.

The current BEHR profiles do not include lightning NO_2, which was part of the motivation for this study. We have added the following sentence to the first section of the discussion:

"These new a priori profiles will correct the absence of modeled lightning NO_2 in the v2.1C a priori profiles."

References

Krotkov, N. A., Lamsal, L. N., Celarier, E. A., Swartz, W. H., Marchenko, S. V., Bucsela, E. J., Chan, K. L., Wenig, M., and Zara, M.: The version 3 OMI NO_2 standard product, Atmos. Meas. Tech., 10, 3133–3149, doi:10.5194/amt-10-3133-2017, URL `https://www.atmos-meas-tech.net/10/3133/2017/`, 2017.

Travis, K. R., Jacob, D. J., Fisher, J. A., Kim, P. S., Marais, E. A., Zhu, L., Yu, K., Miller, C. C., Yantosca, R. M., Sulprizio, M. P., Thompson, A. M., Wennberg, P. O., Crounse, J. D., St. Clair, J. M., Cohen, R. C., Laughner, J. L., Dibb, J. E., Hall, S. R., Ullmann, K., Wolfe, G. M., Pollack, I. B., Peischl, J., Neuman, J. A., and Zhou, X.: Why do models overestimate surface ozone in the Southeast United States?, Atmos. Chem. Phys., 16, 13 561–13 577, doi:10.5194/acp-16-13561-2016, URL `https://www.atmos-chem-phys.net/16/13561/2016/`, 2016.

Quantification of the effect of modeled lightning NO_2 on UV-visible air mass factors

Response to Anonymous Referee #2

Joshua L. Laughner and Ronald C. Cohen

October 4, 2017

We thank the reviewer for their detailed reading of the paper. Below, we address each concern individually. The reviewer's comments will be shown in red, our response in blue, and changes made to the paper are shown in black block quotes. Unless otherwise indicated, page and line numbers correspond to the original paper. Figures, tables, or equations referenced as "Rn" are numbered within this response; if these are used in the changes to the paper, they will be replaced with the proper number in the final paper. Figures, tables, and equations numbered normally refer to the numbers in the original discussion paper.

I feel that this is a lengthy paper based on very limited research. Large part of the discussion on scattering weights may be a self-educating piece for the authors. The discussion section (Section 4) is either inconclusive or conclusions drawn based on limited research. Due to several major concerns I do not think this paper, in the current form, would add any significant insights to the AMT readership.

We respectfully disagree with the reviewer's conclusion that this paper does not add significant insights to the AMT readership. While the conclusion that the presence or absence of lightning NO_2 in the a priori profiles significantly affects the tropospheric AMFs may not be a surprising result, we know of no other work that has explicitly demonstrated this effect, especially in retrievals using high spatial resolution chemical transport models. Goldberg et al. (2017) considered lightning as a possible cause for the difference between GMI and CMAQ UT NO_2 profiles, but did not explicitly demonstrate the effect of varying lightning NO_x emissions in the CTM.

We believe that the detailed discussion of the scattering weights helps the reader understand the changes to the AMFs under different conditions shown in Fig. 2.

For the discussion, we recognize that ending the first two subsections with caveats may take away from the stronger conclusion presented in the first paragraph of each subsection. We have reordered these two subsections to place the stronger conclusion at the end of each section.

1) Lightning NOx emissions vary strongly both spatially and seasonally. Therefore, retrievals are affected differently for various seasons. Conclusions drawn from $\sim$ 1 month in late-spring/early-summer will most likely be incomplete and misleading. I strongly recommend expanding this analysis over the continental US (analyzing urban vs. rural, east vs.

west, north vs. south, etc.) for all months. It would be more instructive if this could be discussed in global context.

We appreciate the reviewer's interest in understanding the effects on lightning NO_2 in broader regions and time periods. Our goal at this time was to first verify that, at a time and place where lightning activity is expected, that the impact on high-resolution a priori profiles is significant and to identify a model configuration that produces a good representation of lightning NO_2 in the a priori profiles. For that reason, we chose to focus on a spatial domain and time period where in situ observations were available in the form of the DC3 campaign. We intend to apply the lessons learned here to the next generation of the BEHR retrieval.

To avoid giving the impression that quantitative results apply without exception to other time periods, we have made the following changes. In the abstract:

> "...Focusing on **late spring and early summer in** the central and eastern United States, we find that a simulation without lightning..."

In the first section of the discussion:

> "...the presence or absence of lightning NO_2 in the a priori profiles has a large effect on the retrieval AMFs in clear-sky conditions which are used to obtain information about boundary layer NO_x (e.g. Lamsal et al., 2010; Beirle et al., 2011; Valin et al., 2013; Lamsal et al., 2015; Lu et al., 2015; Liu et al., 2016, 2017). **Since many of these studies focus on summer months when thunderstorms are common over the US (Barth et al., 2015), the inclusion of lightning NO_2 in the a priori profiles is necessary to accurately constrain the emissions. Lightning is less frequent in wintertime, but the southeast US does experience winter lightning (Orville et al., 2001; Hunter et al., 2001). Therefore, wintertime retrievals will likely see significantly less but nonzero impact from the inclusion of lightning NO_2 in the a priori profiles. Future work will verify this as new a priori profiles are planned for inclusion in the next generation of the BEHR retrieval.**"

In the conclusion:

> "...we find that the effect on the AMF is very regionally dependent. **For summertime retrievals, changing** from profiles using 0 mol NO $flash^{-1}$ to 500 mol NO $flash^{-1}$ shows the largest increase in the AMF..."

Regarding global context, recent work (e.g. Cooper et al., 2014; Nault et al., 2017) suggests that regionally-specific lightning parameterizations are necessary to accurately capture the behavior of lightning around the world. We hope that our work helps other groups developing high resolution retrievals understand the magnitude of the sensitivity of NO_2 retrievals to lightning NO_2 and presents an approach to quantify the uncertainty due to the model's lightning parameterization as in situ observations to compare against become available in other regions.

2) Model vs measurements discrepancies for the upper tropospheric NO2 are bundled solely to lightning NOx emissions and therefore are attempted to address by using a fixed NO mol/flash. There are wide varieties of estimates in the literature, going as low as a factor of 5 lower than the estimate used in this paper. I think, the authors should perform similar analysis with additional simulations for confidence in the presented results.

From Table 2, we can see that the AMFs calculated using the free tropospheric hybrid profiles from the 500 and 665 unnudged mol flash^{-1} simulations bracket the AMF calculated from the average DC3 profile, while the simulation with 0 mol flash^{-1} yields an AMF 35% low. Since the increase in AMF with lightning emissions is approximately linear, this suggests that lower mol flash^{-1} values will underestimate the AMF compared to the DC3 profile; e.g. a simulation using 250 mol flash^{-1} would likely produce an AMF ≈ 1.3.

This is further borne out by the profiles in Fig. 5, where it is apparent that increasing the lightning emissions from 0 to 500 to 665 mol flash^{-1} scales the entire profile above $\sim$ 800 hPa. Profiles with fewer mol flash^{-1} will have a shape in between the 0 and 500 mol flash^{-1} profiles. Since reducing the UT component of the profile reduces the AMF, these simulations will produce worse agreement with the DC3-derived AMF.

Finally, the 500 mol flash^{-1} nudged run with the base flash rate (approximately half that of the unnudged run, Fig. S3) also demonstrates that lower lightning emissions produces a worse agreement with the DC3-derived AMF, since in the fixed mol flash^{-1} approximation, halving the flash rate is equivalent to halving the mol flash^{-1}. Table 2 clearly shows that this run yields an AMF of 1.29, as expected for halving the lightning NO_2. Therefore, we do not believe that adding additional runs with lower mol flash^{-1} values would add value to this work.

I am also concerned by the incomprehensive nature of this analysis. The BEHR algorithm is based on several inputs from the operational OMNO2 products, for instance the use of stratospheric NO2 estimates from OMNO2 for calculating tropospheric slant column amount. Modulation of upper tropospheric NO2 should lead to different estimates for stratospheric NO2. Could you do your own stratosphere-troposphere separation and quantify the effect on both stratospheric and tropospheric NO2 estimates?

While we agree that evaluating the impact of using a high spatial resolution model in the stratospheric separation could be interesting, we do not expect the impact to be significant. In Bucsela et al. (2013) (Fig. 2d), most of the continental US (including the southeast where our analysis sees the largest effect of lightning NO_2) is already masked during the initial stratospheric separation, since the a priori tropospheric column exceeds the threshold for tropospheric contamination, even at the $2^\circ \times 2.5^\circ$ resolution of the model used. As a quick test, we plotted where our WRF-Chem a priori would exceed the 3×10^{14} molec. cm^{-2} threshold for tropospheric contamination from Bucsela et al. (2013) (Fig. R1. The pattern is broadly similar to the masked area in Fig. 2d of Bucsela et al. (2013).

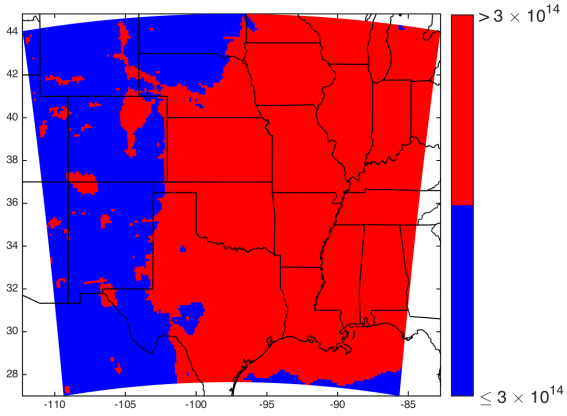

Figure R1: Binary map of the average WRF-Chem tropospheric columns between 1700 and 2200 UTC; red indicates columns greater than the 3×10^{14} molec. cm^{-2} threshold for tropospheric contamination from Bucsela et al. (2013)

Minor comments

Page 2, lines 27-33: Wouldnt the lifetime of NOx vary with altitude? Suggesting the upper tropospheric NOx lifetime < 4 days might be misleading.

Estimates of NO_x lifetime in the outflow of convection have typically assumed that NO_x lifetime was controlled by dilution and nitric acid formation, giving a lifetime of 2–8 days (Schumann and Huntrieser, 2007). However, more recent work from the DC3 campaign has identified that peroxy radicals formed by reactions of organic precurors lofted from the boundary layer by deep convection lead to rapid formation of alkyl-, peroxy-, and multifunctional- nitrate species in the near field of thunderstorms, indicating that UT NO_x lifetime in the outflow of thunderstorms is shorter than previously assumed (Nault et al., 2016, 2017).

We have added text acknowledging the previous assumption of longer lifetime and explaining in more detail the reason for the shorter lifetime proposed:

> "In the upper troposphere, NO_x lifetime has previously been assumed to be long (2–8 days Schumann and Huntrieser, 2007). Recently, work from the Deep Convective Clouds and Chemistry (DC3) campaign showed that the lifetime of NO_x is short near thunderstorms due to active alkyl-, peroxy-, and multifunctional-nitrate chemistry with peroxy radicals formed in the near field from organic precursors lofted from the boundary layer ($\sim$ 3 h Nault et al., 2016), but longer (12–48 h Nault et al., 2016) away from thunderstorms once these radical species are consumed and other controlling factors take over (Bertram et al., 2007; Apel et al., 2012). In either case, lightning NO_x can affect upper tropospheric NO_x concentrations distant from active storms..."

Page 4, line 17, Section 2.3: What is the altitude range of DC3 measurements? Discuss

how you treat simulated profile beyond the range of DC3 measurements.

DC3 measurements cover the range 980 to 178 hPa. We added the following to Section 2.3:

> "Matching the vertical position in this way inherently restricts the model data to the vertical range of the observations."

And to section 2.5.2:

> "When using the DC3-WRF matched profiles (Sect. 2.3), the two greatest surface pressures (1013 and 989) will have essentially no difference, as the matched profiles only extend down to 990 hPa."

Page 5, line 19: How was the estimate of ghost column made? Does this mean, you add a-priori-derived NO2 columns below the cloud to the retrieved tropospheric columns? How does this approach compare with the operational (DOMINO, OMNO2) procedures?

We have added the following text at p. 5, l. 19:

> "The ghost column was estimated by using as the AMF the ratio of the visible modeled slant column (derived from the a priori NO_2 profile, scattering weights, and radiance cloud fraction) to the total modeled tropospheric vertical column. Thus, dividing the observed slant column by this AMF produced a total tropospheric vertical column via a multiplicative correction. This approach is identical to that described in Boersma et al. (2002)."

As mentioned at the end of the above quote, this approach is that described in the OMNO2 Theoretical Basis Document (Boersma et al., 2002). This is indeed the method used in the NASA Standard Product (E. Bucsela, private communication).

Page 5, line 24: What is the logic behind using the fixed tropopause pressure at 200 hPa? Does that mean the BEHR NO2 columns represent columns below 200 hPa? How do you deal with possible errors from using OMNO2-based stratospheric NO2 columns that is likely based on (variable) meteorology-based tropopause pressures?

The 200 hPa upper limit is retained from the original NASA SP v1 approach, where the troposphere profiles end a 200 mbar (Bucsela et al., 2006). Bucsela et al. (2013) indicates that different definitions of the tropopause are expected to have little effect on the retrieval. In any case, since the results presented here focus on differences among AMFs all calculated with 200 hPa as the upper integration limit, much of the effect of the tropopause definition will be canceled out by the difference, since its effects are likely systematic over the time period studied.

Page 6, Eqn 4: Here and everywhere else in the text. This should be tropospheric AMF, not total AMF. Correct or clarify this.

Clarified in text, in Eq. 4 and 5 changed to AMF_{trop}.

Page 6, line 16: Use of black-sky albedo instead of Lambert-Equivalent Reflectivity (LER) should be a large source of errors. Please comment on this based on some recent publications (e.g. Lin et al., 2015; Vasilkov et al., 2017).

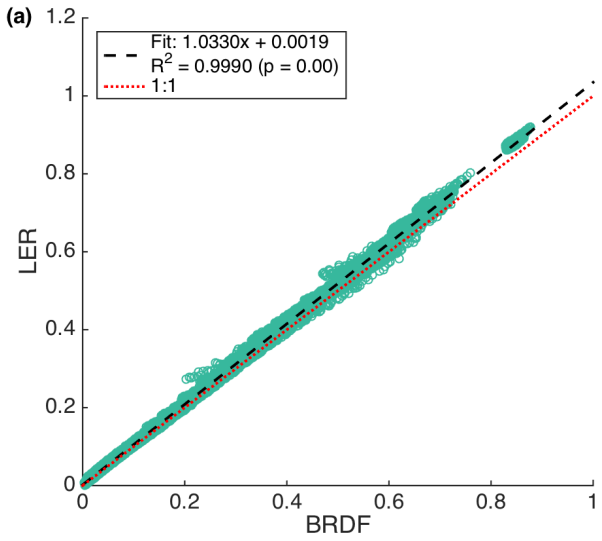

Figure R2: LER surface reflectance calculating using the SCIATRAN model and the method of Vasilkov et al. (2017) with the MODIS MCD43C1 BRDF product compared against surface reflectance calculated directly from the MODIS MCD43C1 BRDF coefficients and the kernels described in Stahler et al. (1999) for 1 day per month for a year for 85 sites across the continental US. The black dashed line is a reduced major axis regression; the fit indicates only a $\sim 3\%$ difference on average.

The differences found in Lin et al. (2015) and Vasilkov et al. (2017) aren't solely due to the difference between an LER and black-sky albedo; both investigated the difference between a climatological surface reflectance with no directional dependence (e.g. OMLER) and a higher spatial resolution, temporally varying BRDF product that does account for the directional dependence of surface reflectivity.

In response to studies such as Vasilkov et al. (2017), we are already working on switching from a black-sky albedo product to the MODIS BRDF product in the next version of the BEHR retrieval. We examined whether calculating an LER was necessary or if using the surface reflectance computed from the MODIS BRDF parameters was sufficient by computing both for one day from each month for 85 sites across the US, spanning urban, power plant, and rural location. Using the method from Vasilkov et al. (2017), we see only a 3% difference using the LER on average (Fig. R2). While the reviewer is correct to point out the importance of the surface reflectance product, it is not relevant for this paper, as our goal is to isolate the effect of lightning NO_2 in a retrieval with high spatial resolution a priori NO_2 profiles.

Page 6, line 18-20: Will this approach capture the seasonal variation of surface pressure? How big is its effect on AMF?

From a WRF-Chem simulation of 2012, the average difference in meteorological surface pressure between June and January does not exceed 15 hPa (1.5% of 1013 hPa). From the AMF sensitivity test of the average WRF 500 mol flash^{-1} (unnudged) profile, by randomly sampling the effect of a 15 hPa change in surface pressure at 10,000 points, we find that is

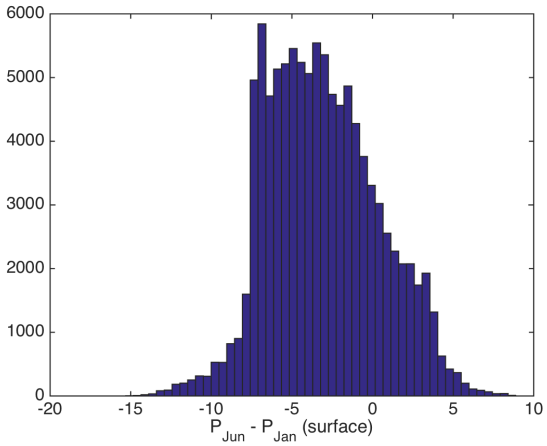

Figure R3: Average difference in surface pressure for all WRF model grid cells between Jan and June 2012.

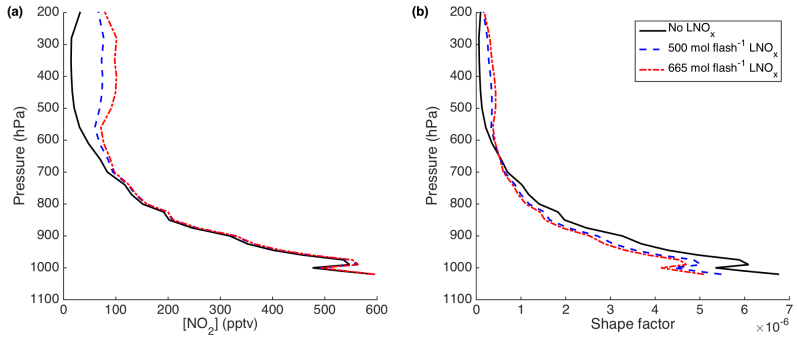

Figure R4: Domain-wide mean WRF-Chem NO_2 profiles. (a) profiles in mixing ratios; (b) profiles in shape factor as defined in Palmer et al. (2001), i.e. number density divided by VCD.

produces only a $\sim 2\%$ average difference in AMF.

Page 6, line 22: OMI cloud fraction.... Is this "effective" or "radiative" cloud fraction?
This is the geometric, a.k.a. effective cloud fraction. Corrected.

Page 6-7, Section 2.5.2: Related to Surface pressure (cloudy). I cannot understand the logic of having different surface pressures for clear and cloudy pixels? Should not this be cloud pressure instead?
In the calculation of cloudy pixel scattering weights, the cloud pressure is treated as the surface pressure. We have edited this section to make this clearer.

Page 8, Figure 1: Please, also include profile shapes which might be more relevant for AMF.
Added (see Fig. R4)

Page 9, lines: 1:3: This discussion is confusing. Should not the effect be based on the altitude of lightning generated NOx?

This discussion is focused on the effect of lesser (higher altitude) surface pressure among the three profiles presented in Fig. 1. Among those three profiles, the altitude of the emitted lightning NO_2 does not change; only the amount of lightning NO_2 varies. In general, yes, the altitude of lightning emission will change the specific behavior, but in the specific simulations being discussed here, the lightning emissions significantly affect the profile above $\sim$ 860 hPa.

Page 10, line 2: In obscure the surface NO2. . ., dont you mean below cloud?

No; a cloud will always, by definition, obscure the below cloud NO_2, our point is that clouds are almost always high enough to hide the part of the NO_2 profile influenced by surface emissions, and so under cloudy conditions, the entire visible part of our modeled profile is influenced by lightning emissions. We have clarified this as:

> "...the cloud is at sufficiently high elevation to obscure **the part of the NO_2 profile influenced by surface emissions**, and therefore restricts..."

Page 16, Section 4.1: What is the message of this section? Why mention nudging at all in the paper if understanding of the 50% decrease in the flash rates by activating FDDA nudging is beyond the scope of the paper?

Laughner et al. (2016) showed that the day-to-day variation in NO_2 profiles driven by changes in wind direction has significant effects on the retrieved NO_2 and especially on top-down emissions constraints using the exponentially modified gaussian method (Beirle et al., 2011; Valin et al., 2013; Lu et al., 2015; Liu et al., 2016, 2017). Consequently, constraining the WRF meteorology using FDDA nudging is an essential part of producing accurate a priori profiles, and our tests showed that including FDDA nudging also affects the lightning flash rates. Therefore, any model optimization intended to produce high resolution a priori NO_2 profiles with lightning emissions should be done with FDDA nudging (or its equivalent in other models) enabled. The discussion with respect to Wong et al. (2013) points out that we do not know that the lower flash rate produced by FDDA nudging is wrong, just that the resultant NO_2 profile has poorer agreement than one produced with greater flash rates. We have added the following text to clarify this:

> "A full analysis of the reason that activating FDDA nudging causes the flash rates to decrease by 50% in our case is beyond the scope of this paper. **Empirically, we see that the NO_2 profile generated by the FDDA run with 1x the base flash rate has less UT NO_2 than was observed during DC3 (Fig. 5). Therefore, we cannot say whether this discrepancy in the profile is due to the reduced number of flashes or a too-low average number of moles of NO emitted per flash. Our correction of doubling the nudged flash rate to improve agreement between the modeled and observed profiles was the most straightforward based on the differences between the nudged and unnudged runs.**"

Page 16, line 22: In less UT NO2 that => less UT NO2 than

Corrected, thank you.

Page 16, Section 4.2: To estimate uncertainty in cloud slicing, Choi et al. 2014 might have conducted more comprehensive analysis, considering errors in cloud and other parameters.
We have added text acknowledging this possibility:

> "Since Choi et al. (2014) used a typical C-shaped NO_2 profile that included lightning NO_2 (e.g. Pickering et al., 1998), based on our results, we expect that any uncertainty should be closer to the difference we observed between the 500 and 665 mol flash^{-1} profiles, $\leqslant 1\%$, **although we note that the analysis in Choi et al. (2014) may include additional sources of uncertainty not captured by our work.**"

References

Apel, E. C., Olson, J. R., Crawford, J. H., Hornbrook, R. S., Hills, A. J., Cantrell, C. A., Emmons, L. K., Knapp, D. J., Hall, S., Mauldin III, R. L., Weinheimer, A. J., Fried, A., Blake, D. R., Crounse, J. D., Clair, J. M. S., Wennberg, P. O., Diskin, G. S., Fuelberg, H. E., Wisthaler, A., Mikoviny, T., Brune, W., and Riemer, D. D.: Impact of the deep convection of isoprene and other reactive trace species on radicals and ozone in the upper troposphere, Atmos. Chem. Phys., 12, 1135–1150, doi:10.5194/acp-12-1135-2012, URL `http://www.atmos-chem-phys.net/12/1135/2012/`, 2012.

Barth, M. C., Cantrell, C. A., Brune, W. H., Rutledge, S. A., Crawford, J. H., Huntrieser, H., Carey, L. D., MacGorman, D., Weisman, M., Pickering, K. E., Bruning, E., Anderson, B., Apel, E., Biggerstaff, M., Campos, T., Campuzano-Jost, P., Cohen, R., Crounse, J., Day, D. A., Diskin, G., Flocke, F., Fried, A., Garland, C., Heikes, B., Honomichl, S., Hornbrook, R., Huey, L. G., Jimenez, J. L., Lang, T., Lichtenstern, M., Mikoviny, T., Nault, B., O'Sullivan, D., Pan, L. L., Peischl, J., Pollack, I., Richter, D., Riemer, D., Ryerson, T., Schlager, H., Clair, J. S., Walega, J., Weibring, P., Weinheimer, A., Wennberg, P., Wisthaler, A., Wooldridge, P. J., and Ziegler, C.: The Deep Convective Clouds and Chemistry (DC3) Field Campaign, Bull. Am. Met. Soc., 96, 1281–1309, doi: 10.1175/bams-d-13-00290.1, 2015.

Beirle, S., Boersma, K., Platt, U., Lawrence, M., and Wagner, T.: "Megacity Emissions and Lifetimes of Nitrogen Oxides Probed from Space", Science, 333, 1737–1739, 2011.

Bertram, T. H., Perring, A. E., Wooldridge, P. J., Crounse, J. D., Kwan, A. J., Wennberg, P. O., Scheuer, E., Dibb, J., Avery, M., Sachse, G., Vay, S. A., Crawford, J. H., McNaughton, C. S., Clarke, A., Pickering, K. E., Fuelberg, H., Huey, G., Blake, D. R., Singh, H. B., Hall, S. R., Shetter, R. E., Fried, A., Heikes, B. G., and Cohen, R. C.: Direct Measurements of the Convective Recycling of the Upper Troposphere, Science, 315, 816–820, doi:10.1126/science.1134548, 2007.

Boersma, K., Bucsela, E., Brinksma, E., and Gleason, J.: NO_2, in: OMI Algorithm Theoretical Basis Document, vol 4, OMI Trace Gas Algorithms, ATB-OMI-04, version 2.0, pp.

13–36, URL http://eospso.nasa.gov/sites/default/files/atbd/ATBD-OMI-04.pdf, 2002.

Bucsela, E., Krotkov, N., Celarier, E., Lamsal, L., Swartz, W., Bhartia, P., Boersma, K., Veefkind, J., Gleason, J., and Pickering, K.: "A new tropospheric and stratospheric NO_2 retrieval algorithm for nadir-viewing satellite instruments: applications to OMI, Atmos. Meas. Tech., 6, 2607–2626, doi:10.5194/amt-6-2607-2013, 2013.

Bucsela, E. J., Celarier, E. A., Wenig, M. O., Gleason, J. F., Veefkind, J. P., Boersma, K. F., and Brinksma, E. J.: Algorithm for NO_2 vertical column retrieval from the ozone monitoring instrument, IEEE T. Geosci. Remote, 44, 1245–1258, doi:10.1109/TGRS.2005.863715, 2006.

Choi, S., Joiner, J., Choi, Y., Duncan, B. N., Vasilkov, A., Krotkov, N., and Bucsela, E.: First estimates of global free-tropospheric NO_2 abundances derived using a cloud-slicing technique applied to satellite observations from the Aura Ozone Monitoring Instrument (OMI), Atmos. Chem. Phys., 14, 10 565–10 588, doi:10.5194/acp-14-10565-2014, URL http://www.atmos-chem-phys.net/14/10565/2014/, 2014.

Cooper, M., Martin, R. V., Wespes, C., Coheur, P.-F., Clerbaux, C., and Murray, L. T.: Tropospheric nitric acid columns from the IASI satellite instrument interpreted with a chemical transport model: Implications for parameterizations of nitric oxide production by lightning, J. Geophys. Res. Atmos., 119, 10 068–10 079, doi:10.1002/2014JD021907, URL http://dx.doi.org/10.1002/2014JD021907, 2014.

Goldberg, D. L., Lamsal, L. N., Loughner, C. P., Swartz, W. H., Lu, Z., and Streets, D. G.: A high-resolution and observationally constrained OMI NO_2 satellite retrieval, Atmos. Chem. Phys., 17, 11 403–11 421, doi:10.5194/acp-17-11403-2017, URL https://www.atmos-chem-phys.net/17/11403/2017/, 2017.

Hunter, S. M., Underwood, S. J., Holle, R. L., and Mote, T. L.: Winter Lightning and Heavy Frozen Precipitation in the Southeast United States, Weather Forecasting, 16, 478–490, doi:10.1175/1520-0434(2001)016⟨0478:wlahfp⟩2.0.co;2, URL https://doi.org/10.1175/1520-0434(2001)016<0478:wlahfp>2.0.co;2, 2001.

Lamsal, L. N., Martin, R. V., van Donkelaar, A., Celarier, E. A., Bucsela, E. J., Boersma, K. F., Dirksen, R., Luo, C., and Wang, Y.: Indirect validation of tropospheric nitrogen dioxide retrieved from the OMI satellite instrument: Insight into the seasonal variation of nitrogen oxides at northern midlatitudes, J. Geophys. Res. Atmos., 115, doi:10.1029/2009JD013351, 2010.

Lamsal, L. N., Duncan, B. N., Yoshida, Y., Krotkov, N. A., Pickering, K. E., Streets, D. G., and Lu, Z.: U.S. NO_2 trends (20052013): EPA Air Quality System (AQS) data versus improved observations from the Ozone Monitoring Instrument (OMI), Atmos. Environ., 110, 130–143, doi:10.1016/j.atmosenv.2015.03.055, 2015.

Laughner, J. L., Zare, A., and Cohen, R. C.: Effects of daily meteorology on the interpretation of space-based remote sensing of NO_2, Atmospheric Chemistry and Physics,

16, 15 247–15 264, doi:10.5194/acp-16-15247-2016, URL http://www.atmos-chem-phys.net/16/15247/2016/, 2016.

Lin, J.-T., Liu, M.-Y., Xin, J.-Y., Boersma, K. F., Spurr, R., Martin, R., and Zhang, Q.: Influence of aerosols and surface reflectance on satellite NO_2 retrieval: seasonal and spatial characteristics and implications for NO_x emission constraints, Atmos. Chem. Phys., 15, 11 217–11 241, doi:10.5194/acp-15-11217-2015, 2015.

Liu, F., Beirle, S., Zhang, Q., Dörner, S., He, K., and Wagner, T.: NOx lifetimes and emissions of cities and power plants in polluted background estimated by satellite observations, Atmos. Chem. Phys., 16, 5283–5298, doi:10.5194/acp-16-5283-2016, 2016.

Liu, F., Beirle, S., Zhang, Q., van der A, R. J., Zheng, B., Tong, D., and He, K.: NO_x emission trends over Chinese cities estimated from OMI observations during 2005 to 2015, Atmos. Chem. Phys. Discuss., pp. 1–21, doi:10.5194/acp-2017-369, 2017.

Lu, Z., Streets, D., de Foy, B., Lamsal, L., Duncan, B., and Xing, J.: "Emissions of nitrogen oxides from US urban areas: estimation from Ozone Monitoring Instrument retrievals for 2005–2014", Atmos. Chem. Phys., 15, 10 367–10 383, doi:10.5194/acp-15-10367-2015, 2015.

Nault, B. A., Garland, C., Wooldridge, P. J., Brune, W. H., Campuzano-Jost, P., Crounse, J. D., Day, D. A., Dibb, J., Hall, S. R., Huey, L. G., Jimenez, J. L., Liu, X., Mao, J., Mikoviny, T., Peischl, J., Pollack, I. B., Ren, X., Ryerson, T. B., Scheuer, E., Ullmann, K., Wennberg, P. O., Wisthaler, A., Zhang, L., and Cohen, R. C.: Observational Constraints on the Oxidation of NOx in the Upper Troposphere, J. Phys. Chem. A, 120, 1468–1478, doi:10.1021/acs.jpca.5b07824, 2016.

Nault, B. A., Laughner, J. L., Wooldridge, P. J., Crounse, J. D., Dibb, J., Diskin, G., Peischl, J., Podolske, J. R., Pollack, I. B., Ryerson, T. B., Scheuer, E., Wennberg, P. O., and Cohen, R. C.: Lightning NO_x Emissions: Reconciling Measured and Modeled Estimates With Updated NO_x Chemistry, Geophys. Res. Lett., doi:10.1002/2017GL074436, 2017.

Orville, R. E., Huffines, G., Nielsen-Gammon, J., Zhang, R., Ely, B., Steiger, S., Phillips, S., Allen, S., and Read, W.: Enhancement of cloud-to-ground lightning over Houston, Texas, Geophys. Res. Lett., 28, 2597–2600, doi:10.1029/2001GL012990, URL http://dx.doi.org/10.1029/2001GL012990, 2001.

Palmer, P., Jacob, D., Chance, K., Martin, R., Spurr, R., Kurosu, T., Bey, I., Yantosca, R., Fiore, A., and Li, Q.: "Air mass factor formulation for spectroscopic measurements from satellites: Applications to formaldehyde retrievals from the Global Ozone Monitoring Experiment", J. Geophys. Res. Atmos., 106, 14 539–14 550, 2001.

Pickering, K. E., Wang, Y., Tao, W.-K., Price, C., and Müller, J.-F.: J. Geophys. Res., 103, 31 203–31 216, 1998.

Schumann, U. and Huntrieser, H.: The global lightning-induced nitrogen oxides source, Atmos. Chem. Phys., 7, 3823–3907, 2007.

Stahler, A., Lucht, W., Schaaf, C., Tsang, T., Gao, F., Li, X., Muller, J.-P., Lewis, P., Barnsley, M., Strugnell, N., Hu, B., Hyman, A., d'Entremont, R., Chen, L., Liu, Y., McIver, D., Liang, S., Disney, M., Hobson, P., Dunderdale, M., and Roberts, G.: MODIS BRDF/Albedo Product: Algorithm Theoretical Basis Document Version 5.0, p. 16, URL http://modis.gsfc.nasa.gov/data/atbd/atbd_mod09.pdf, 1999.

Valin, L., Russell, A., and Cohen, R.: "Variations of OH radical in an urban plume inferred from NO_2 column measurements", Geophys. Res. Lett., 40, 1856–1860, doi:10.1002/grl.50267, 2013.

Vasilkov, A., Qin, W., Krotkov, N., Lamsal, L., Spurr, R., Haffner, D., Joiner, J., Yang, E.-S., and Marchenko, S.: Accounting for the effects of surface BRDF on satellite cloud and trace-gas retrievals: a new approach based on geometry-dependent Lambertian equivalent reflectivity applied to OMI algorithms, Atmos. Meas. Tech., 10, 333–349, doi:10.5194/amt-10-333-2017, URL https://www.atmos-meas-tech.net/10/333/2017/, 2017.

Wong, J., Barth, M. C., and Noone, D.: Evaluating a lightning parameterization based on cloud-top height for mesoscale numerical model simulations, Geosci. Model Dev., 6, 429–443, doi:10.5194/gmd-6-429-2013, 2013.

Quantification of the effect of modeled lightning NO_2 on UV-visible air mass factors

Joshua L. Laughner[1] and Ronald C. Cohen[1,2]

[1]Department of Chemistry, University of California, Berkeley, Berkeley, CA 94720
[2]Department of Earth and Planetary Sciences, University of California, Berkeley, Berkeley, CA 94720

Correspondence to: R.C. Cohen (rccohen@berkeley.edu)

Abstract. Space-borne measurements of tropospheric nitrogen dioxide (NO_2) columns are up to 10x more sensitive to upper tropospheric NO_2 than near-surface NO_2 over low reflectivity surfaces. Here, we quantify the effect of adding simulated lightning NO_2 to the a priori profiles for NO_2 observations from the Ozone Monitoring Instrument using modeled NO_2 profiles from the Weather Research and Forecasting—Chemistry (WRF-Chem) model. With observed NO_2 profiles from the Deep Convective Clouds and Chemistry (DC3) aircraft campaign as observational truth, we quantify the bias in the NO_2 column that occurs when lightning NO_2 is not accounted for in the a priori profiles. Focusing on late spring and early summer in the central and eastern United States, we find that a simulation without lightning NO_2 underestimates the air mass factor (AMF) by ~~26~~25% on average for common summer OMI viewing geometry, and 35% for viewing geometries that will be encountered by geostationary satellites. Using a simulation with 500 to 665 mol NO flash^{-1} produces good agreement with observed NO_2 profiles and reduces the bias in the AMF to $< \pm 4\%$ for OMI viewing geometries. The bias is regionally dependent, with the strongest effects in the southeast United States (up to 80%) and negligible effects in the central US. We also find that constraining WRF meteorology to a reanalysis dataset reduces lightning flash counts by a factor of 2 compared to an unconstrained run, most likely due to changes in the simulated water vapor profile.

1 Introduction

NO_x ($\equiv$ NO + NO_2) is a short-lived (typical summer lifetime 2–7 h) trace gas in the atmosphere. NO_x is emitted by both anthropogenic and natural processes; the former is primarily due to combustion, while the latter includes biomass burning, soil bacteria nitrification or denitrification, and lightning. NO_x regulates ozone production throughout the troposphere; therefore accurate measurements of NO_x and understanding of NO_x chemistry is essential to describe and predict the role of ozone as both an air quality hazard, oxidant, and a greenhouse gas.

Space-borne measurements of NO_2 as an indicator of total NO_x, such as those from the Global Ozone Monitoring Experiment (GOME and GOME-2), SCanning Imaging Absorption SpectroMeter for Atmospheric CHartographY (SCIAMACHY), and Ozone Monitoring Instrument (OMI) are a valuable tool in understanding NO_x emissions and chemistry because of their global reach and long data records. Use of these observations includes assessment of NO_x chemistry (e.g. Beirle et al., 2011; Valin et al., 2013) anthropogenic emissions (e.g. Miyazaki et al., 2012; Russell et al., 2012; Lu et al., 2015; Liu et al., 2016,

2017) and natural emissions (e.g. Martin et al., 2007; Beirle et al., 2011; Hudman et al., 2012; Mebust et al., 2011; Mebust and Cohen, 2013, 2014; Miyazaki et al., 2014; Zörner et al., 2016).

Retrieval of tropospheric NO_2 from a UV-visible satellite spectrometer requires three main steps: fitting the measured absorbance to produce a slant column density (SCD), separation of the stratospheric and tropospheric signals, and conversion of the tropospheric SCD to a vertical column density (Boersma et al., 2011; Bucsela et al., 2013). This final step accounts for the effect of variable path length through the atmosphere, surface elevation and reflectance, and the vertical distribution of NO_2 (Palmer et al., 2001). For observations over low reflectivity surfaces, the sensitivity of the satellite to NO_2 decreases towards the surface, as photons penetrating into the lower atmosphere may scatter into the surface, where most are absorbed; thus, there is a higher probability that a photon that reaches the detector has interacted only with the higher levels of the atmosphere (Hudson et al., 1995; Richter and Wagner, 2011). That is to say, a given number of NO_2 molecules in the upper troposphere produce a greater signal than the same number of NO_2 molecules at the surface would. Thus, a priori knowledge of the vertical profile of NO_2 is necessary to account for this effect in the retrieval.

These vertical profiles are simulated using chemical transport models (CTMs) such as TM4 (used in Boersma et al., 2011), the Global Modeling Initiative CTM (used in Bucsela et al., 2013), or the Weather Research and Forecasting—Chemistry (WRF-Chem, used in Russell et al., 2011). These models must account for atmospheric transport, chemistry, emissions, and deposition to accurately simulate the required NO_2 profiles. Most emission of NO_2 occurs at or very near the surface. There are comparatively weaker sources of NO_2 in the upper troposphere, limited to transport from the surface, aircraft, stratospheric mixing, and lightning (Jaeglé et al., 1998).

Simulation of lightning NO_x emission in these models is typically done by assuming each flash emits a set number of molecules of NO. The number and location of lightning flashes is often parameterized using the method of Price and Rind (1992), which relates lightning flash rates to cloud top heights, which in turn are calculated from the model's meteorology. In CTMs focused on simulating surface chemistry to understand or predict air quality, such as WRF-Chem or the Community Multi-scale Air Quality (CMAQ) model, including NO_x produced by lightning may be disabled by default or require the user to prepare additional input files. As these models are often used to simulate high resolution a priori profiles (e.g. Russell et al., 2011, 2012; Kuhlmann et al., 2015; Laughner et al., 2016; Goldberg et al., 2017), the absence of lightning NO_x from the a priori profiles may contribute to a significant bias in the interpretation of the measurements (e.g. Travis et al., 2016) .

In the upper troposphere, ~~the~~ NO_x lifetime has previously been assumed to be long (2–8 days, Schumann and Huntrieser, 2007) . Recently, work from the Deep Convective Clouds and Chemistry (DC3) campaign showed that the lifetime of NO_x is short near thunderstorms ~~(~ 3 h Nault et al., 2016) , but longer (12–48 h)~~ due to active alkyl-, peroxy-, and multifunctional- nitrate chemistry with peroxy radicals formed in the near field from organic precursors lofted from the boundary layer (~ 3 h, Nault et al., 2016) , but longer (12–48 h, Nault et al., 2016) away from thunderstorms ~~(Bertram et al., 2007; Apel et al., 2012) . As a result~~once these radical species are consumed and other controlling factors take over (Bertram et al., 2007; Apel et al., 2012) . In either case, lightning NO_x can affect upper tropospheric NO_x concentrations distant from active storms; thus, simulated lightning NO_x will have wide-reaching and persistent effects on a priori NO_2 profiles throughout a model domain. Previous work by, e.g. Beirle et al. (2009) and Pickering et al. (2016), has provided careful analysis of the effect of lightning on AMFs in the

near field of a thunderstorm, with the goal of improving direct satellite measurements of the mean production of NO per flash. Goldberg et al. (2017) compared high resolution NO_2 profiles from the Community Multiscale Air Quality (CMAQ) model with those from a lower resolution Global Modeling Initiative (GMI) model and found that the CMAQ profiles had less upper troposphere (UT) NO_2 than the GMI profiles, despite greater lightning emissions in CMAQ. Our goal here is to consider the broader impact of modeled lightning NO_x on satellite retrievals on the full domain both near and far from the lightning event.

In this work, we evaluate the impact of modeled lightning NO_x on NO_2 a priori profiles simulated with the WRF-Chem chemical transport model for a domain covering the central and eastern US. We first consider the problem in a general sense, with a sensitivity test using three profiles simulated with different amounts of lightning NO_x. We then compare modeled profiles to observations from the ~~Deep Convective Clouds and Chemistry (~~DC3 ~~)~~ campaign to determine the accuracy of AMFs derived using the simulated profiles, and finally implement these profiles in an NO_2 retrieval to demonstrate the spatial pattern and significance of this effect in a real application.

2 Methods

2.1 The Deep Convective Clouds and Chemistry Campaign

The Deep Convection Clouds and Chemistry (DC3) Campaign is an aircraft measurement campaign that took place between 18 May and 22 June 2012 throughout the central and southeastern US (Barth et al., 2015). The NASA DC-8 aircraft sampled outflow from convective systems, studying direct and aged lightning NO_x emissions. We use NO_2 measurements made by laser induced florescence at 1 second resolution in this study (Thornton et al., 2000; Nault et al., 2015).

2.2 Weather Research and Forecasting—Chemistry Model

We use the Weather Research and Forecasting—Chemistry (WRF-Chem) model v. 3.5.1 (Grell et al., 2005) to simulate NO_2 profiles across a domain that covers the same region as the DC3 campaign at 12 km model resolution with 29 vertical levels. Meteorological initial and boundary conditions are driven by the North American Regional Reanalysis (NARR) dataset. Chemical initial and boundary conditions are driven by output from the Model for Ozone and Related chemical Tracers (MOZART; Emmons et al., 2010) provided by the National Center for Atmospheric Research. Anthropogenic emissions are driven by the National Emissions Inventory 2011 (NEI 11); each emitted species is scaled domain-wide by the ratio of its total annual 2012 to 2011 emissions provided by the Environmental Protection Agency (EPA, 2016), e.g. 2012 NO_x emissions are given at 13.657 million tons, 94% of the 2011 value of 14.519 million tons; the gridded 2011 NO emissions are multiplied by 0.94 to obtain 2012 emissions. Biogenic emissions are driven by the Model of Emissions of Gases and Aerosol from Nature (MEGAN; Guenther et al., 2006). The chemical mechanism is a customized version of The Regional Atmospheric Chemistry Model, version 2 (RACM2; Goliff et al., 2013) that includes updates to alkyl nitrate chemistry from Browne et al. (2014) and Schwantes et al. (2015), as well as formation, dissociation and photolysis of methylperoxy nitrate (Browne et al., 2011, see

also http://wiki.seas.harvard.edu/geos-chem/images/GEOS_changes_MPN_chemistry.pdf) Instantaneous values of the model output are sampled every half hour.

WRF can be run such that the meteorology within the domain is driven by the model physics chosen, constrained by reanalysis meteorology data only through the initial and boundary conditions. Alternatively, four dimensional data analysis (FDDA) nudging (Liu et al., 2006) can be used to nudge the model meteorology towards a reanalysis meteorology product throughout the domain. We use this capability in two WRF-Chem simulations, nudging towards the NARR meteorology. In all other simulations, the meteorology evolves according to the model physics.

Lightning NO_x emissions are calculated by the standard modules in WRF-Chem 3.5.1, with a slight modification to the assumed emission profile (described below). The flash rates (number of lightning flashes per unit time) are determined by the Price and Rind level of neutral buoyancy parameterization (Price and Rind, 1992), which depends on cloud top height, calculated using the Grell 3D cumulus physics (Grell, 1993; Grell and Dévényi, 2002) with Lin microphysics (Lin et al., 1983). This number of flashes calculated may be scaled by a constant factor, we use this functionality for one run in Sect. 3.2, otherwise the scaling factor is 1. The intra-cloud/cloud-to-ground ratio is prescribed using the Boccippio et al. (2001) climatology; both intra-cloud and cloud-to-ground flashes are specified to generate the same number of mol NO per flash (Cooray et al., 2009; Ott et al., 2010), which for this study is 0, 500, or 665 mol flash^{-1}. These values are chosen to represent no lightning, the standard midlatitude assumption (500 mol flash^{-1} Hudman et al., 2007), and the recently proposed 33% increase in lightning NO_x emissions of Nault et al. (2017) (665 mol flash^{-1}).

The vertical distribution of NO emissions is driven by a modified version of the profiles from Ott et al. (2010). Several recent studies (Allen et al., 2012; Seltzer et al., 2015) suggest that the standard Ott profiles place too much NO_x in the mid-troposphere. Ott et al. (2010) calculated these profiles using a polynomial fit to profiles of the post-convection vertical distribution of lightning NO_x simulated by a cloud resolving model. The midlatitude profile generated by the cloud resolving model has a bimodal distribution not captured by the polynomial fit; therefore we replace the standard (polynomial fit) Ott et al. (2010) midlatitude profile in WRF-Chem with the bimodal profile.

2.3 Matching aircraft and model data

We match WRF-Chem data to DC3 observations to evaluate the accuracy of the chosen lightning parameterization. Each 1 second DC3 NO_2 observation is paired with the corresponding WRF-Chem data point. Data points are matched in time by finding the WRF-Chem output file (available every half-hour) nearest in time to a given DC3 observation.

Horizontally, a WRF-Chem data point is said to match with a DC3 observation if the latitude and longitude of the DC3 observation lie within the box defined by the midpoints of the WRF-Chem grid cell edges. These midpoints are computed as the average of the relevant corner coordinates (e.g. the western edge point is the average of the northwestern and southwestern corners); the corner coordinates are calculated by assuming that corners not on the edge of the domain are the average of the four surrounding centers. Corners on the domain edge are calculated by extrapolating from the internal corners.

Vertically, we find the matching WRF-Chem data point from the column of such points identified by the previous two steps by finding the WRF-Chem grid point with the smallest difference in pressure compared to the DC3 observation. The result is

two vectors of NO_2 concentrations (DC3 and WRF-Chem) that are the same length; WRF-Chem data points that correspond to multiple DC3 observations are repeated, thus inherently giving them more weight and reflecting the sampling of the aircraft. Matching the vertical position in this way inherently restricts the model data to the vertical range of the observations.

2.4 The Ozone Monitoring Instrument

The Ozone Monitoring Instrument is a polar-orbiting, nadir-viewing UV-visible spectrometer on board the Aura satellite, launched in 2004. It has a nadir pixel size of 13×24 km^2. The primary detector is a 2D CCD array that observes a swath width of 2600 km and a spectral range of 270–500 nm (Levelt et al., 2006). It provides daily global observation for the first three years of operation; after 2007 several detector rows developed anomalous radiances (termed the "row anomaly", http://projects.knmi.nl/omi/research/product/rowanomaly-background.php) that have expanded over time; from July 2011 on, this affects approximately one-third of the pixels. There are two publicly available global products of NO_2 column densities, the KNMI DOMINO product (Boersma et al., 2011) and the NASA Standard Product v3 (Krotkov et al., 2017), and numerous regional products, including OMI-EC (McLinden et al., 2014), Hong Kong OMI NO_2 (Kuhlmann et al., 2015), Peking University OMI NO_2 (POMINO Lin et al., 2015), Empa OMI NO_2 (EOMINO, http://temis.empa.ch/index.php), DOMINO2_GC (Vinken et al., 2014), and the Berkeley High Resolution OMI NO_2 retrieval (Russell et al., 2011, 2012).

2.5 Berkeley High Resolution OMI NO_2 retrieval

2.5.1 Retrieval product

To demonstrate the impact of modeled lightning NO_x on retrieved NO_2 column densities, we use v2.1C of the BErkeley High Resolution (BEHR) NO_2 retrieval. Details of the algorithm are given in Russell et al. (2011); more recent updates are given in the changelog (http://behr.cchem.berkeley.edu/Portals/2/Changelog.txt). This product is available for download at http://behr.cchem.berkeley.edu/DownloadBEHRData.aspx.

Version 2.1C of the BEHR product is based on the NASA Standard Product version 2 (SP v2). It uses the OMI total slant column densities (SCDs) from the OMI NO_2 product OMNO2A v1.2.3 (Boersma et al., 2002; Bucsela et al., 2006, 2013), as well as the stratospheric separation and destriping from the NASA Standard Product v2 ~~.~~(SP v2). Version 3 of the NASA Standard Product was released in 2016, and includes new spectral fitting and tropospheric AMF calculations. The change from SP v2 to v3 does not affect any of the AMF calculations in this work. Krotkov et al. (2017) indicates that the tropospheric VCDs over unpolluted areas are similar between SP v2 and v3, therefore, when effects on retrieved VCDs are considered here, we expect our conclusions to be unaltered when BEHR is updated to use SP v3 data.

The BEHR product recalculates the tropospheric air mass factor (AMF) using the formulation in Palmer et al. (2001). In previous versions of BEHR, the tropospheric AMFs and resulting vertical column densities (VCDs) were always "total" tropospheric columns, i.e., they included an estimated ghost NO_2 column below clouds. The ghost column was estimated by using as the AMF the ratio of the visible modeled slant column (derived from the a priori NO_2 profile, scattering weights, and radiance cloud fraction) to the total modeled tropospheric vertical column. Thus, dividing the observed slant column by this

AMF produced a total tropospheric vertical column via a multiplicative correction. This approach is identical to that described in Boersma et al. (2002) .

Starting in v2.1C, "visible-only" tropospheric AMFs and VCDs are included (which do not include the below-cloud ghost column), in addition to the "total" tropospheric VCDs. In both cases, separate AMFs for clear and cloudy scenes are calculated using Eq. (1)

$$\mathrm{AMF} = \int_{p_0}^{p_{\mathrm{tp}}} w(p) S(p)\, dp \tag{1}$$

where p_0 is the surface or cloud pressure (for clear and cloudy scenes, respectively), p_{tp} is the tropopause pressure (fixed at 200 hPa), $w(p)$ are the pressure-dependent scattering weights from the TOMRAD look-up table used in the NASA SP v2 (Bucsela et al., 2013), which must be corrected for the temperature dependence of the NO_2 cross section:

$$w(p) = w_0(p)\,[1 - 0.003(T(p) - 220)] \tag{2}$$

where $w_0(p)$ is the scattering weight from the look-up table and T is the temperature in Kelvin for a given latitude, longitude, and month; T is taken from the same temperature profiles used in the NASA SP v2 (Bucsela et al., 2013). Recently, an error in the temperature profile lookup for BEHR v2.1C was identified. This caused a $\sim 5\%$ bias in the AMFs, but has been corrected for this study.

Finally, $S(p)$, the shape factor, is computed as:

$$S(p) = \left(\int_{p_s}^{p_{\mathrm{tp}}} g(p)\, dp \right)^{-1} g(p) \tag{3}$$

where $g(p)$ is the NO_2 vertical profile, and p_s is either the surface or cloud pressure, depending on whether a total (visible + ghost) or visible-only tropospheric VCD is desired. BEHR v2.1C provides both. For clear scenes, p_s is always the surface pressure. For cloudy scenes, p_s is the surface pressure when calculating the total tropospheric VCD and the cloud pressure when calculating the visible-only VCD.

The clear and cloudy AMFs for a given pixel are combined as:

$$\mathrm{AMF_{total}}\mathrm{AMF_{trop}} = (1 - f)\mathrm{AMF_{clear}} + f\mathrm{AMF_{cloudy}} \tag{4}$$

where f is the radiance cloud fraction, i.e. the fraction of light from the pixel that is reflected off of clouds. The final VCD is computed as:

$$\mathrm{VCD} = \frac{\mathrm{SCD}}{\mathrm{AMF_{total}}} \frac{\mathrm{SCD}}{\mathrm{AMF_{trop}}} \tag{5}$$

Parameter	Abbreviation	Values	Unit
Solar Zenith Angle	SZA	0, 11, 22, 33, 44, 55, 66, 77, 88	deg.
Viewing Zenith Angle	VZA	0, 14, 28, 42, 56, 70	deg.
Relative Azimuth Angle	RAA	0, 45, 90, 135, 180	deg.
Albedo (clear sky)	Alb	0, 0.009, 0.018, 0.027, 0.036, 0.044, 0.053, 0.062, 0.071, 0.080	unitless
Albedo (cloudy sky)	Alb	0.700, 0.722, 0.744, 0.767, 0.789, 0.811, 0.833, 0.856, 0.878, 0.900	unitless
Surface Pressure (clear)	Surf P	1013, 989, 965, 940, 916, 892, 868, 843, 819, 795	hPa
~~Surface~~ Cloud Pressure (cloudy)	~~Surf~~ Cld P	1003, 930, 857, 783, 710, 637, 564, 490, 417, 344	hPa

Table 1. The values used for the five input parameters to the AMF TOMRAD lookup table in the sensitivity tests. Albedo and surface pressure have different sets of values when the sensitivity test is looking at clear sky and cloudy sky scenarios. For cloudy scenes, the cloud pressure is used as the surface pressure.

where the SCD is the tropospheric slant column density from the NASA SP v2.

The vector of scattering weights, $w(p)$, chosen from the TOMRAD look-up table depends on five parameters: solar zenith angle (SZA), viewing zenith angle (VZA), relative azimuth angle (RAA), albedo, and surface pressure. The SZA, VZA, and RAA are directly provided or can be calculated from data provided in the NASA SP v2. The surface albedo for a given pixel is calculated by averaging the black sky albedo product MCD43C3 (Schaaf and Wang, 2015) values that fall within the pixel. This product is generated by the Moderate Resolution Imaging Spectroradiometer (MODIS) instruments on board the Aqua and Terra satellites. Clouds are assumed to have an albedo of 0.8 (Stammes et al., 2008). Surface pressures are calculated by averaging elevation data from the Global Land One-km Base Elevation project (Hastings and Dunbar, 1999) that falls within the pixel and assuming a scale height of 7.4 km; cloud pressures are from the OMI O2-O2 algorithm (Acarreta et al., 2004; Sneep et al., 2008; Bucsela et al., 2013) and are included in the NASA SP v2.

When averaging over time for the results in Sect. 3.3 we only use pixels with the OMI geometric cloud fraction < 0.2, XTrackQualityFlags = 0, and an even integer for VcdQualityFlags. The averages weight each pixel's contribution by the inverse of the pixel area. Unless otherwise stated, all results in this work use the total tropospheric column.

2.5.2 AMF sensitivity tests

To understand the sensitivity of the AMF to the profile shape under different conditions, we carry out sensitivity tests by varying the five input parameters to the TOMRAD look-up table. Table 1 lists the input parameters and the values used for each parameter. For albedo and surface pressure, two sets of values are used; one represents common values seen for clear (unclouded) scenes, the other cloudy scenes. In cloudy scenes, the cloud pressure is used as the surface pressure. The range of values for SZA, VZA, and RAA span the values defined in the TOMRAD look-up table. The range of values for Albedo (clear sky), Surface Pressure (clear sky), and ~~Surface~~ Cloud Pressure (cloudy) span the average 5th and 95th percentiles of

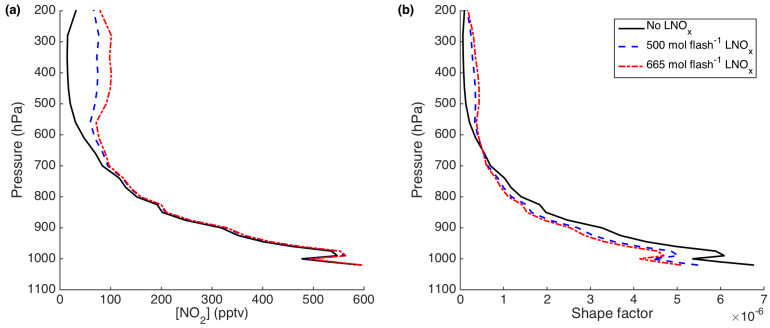

Figure 1. Domain-wide mean WRF-Chem NO_2 profiles. (a) profiles in mixing ratios; (b) profiles in shape factor as defined in Palmer et al. (2001) , i.e. number density divided by VCD.

those values observed in seven days of BEHR data (2012-06-01 to 2012-06-07). The limits for Albedo (cloudy) are chosen as 0.8 ± 0.1, i.e. the assumed cloud albedo plus a reasonable range to explore.

Scattering weights are calculated for every combination of clear or cloudy parameters (27000 combinations). We choose the temperature correction (Sect. 2.5.1, Eq. 2) assuming the June temperature profile at 37.5° N, 95° W. Using a single NO_2 profile, an AMF is calculated for every combination of input parameters.

We use three types of NO_2 vertical profiles for the AMF sensitivity tests.

1. One derived from the 1 sec DC3 NO_2 data (Sect. 2.1)
2. One using WRF-Chem output matched to the DC3 flight path (Sect. 2.3)
3. One using WRF-Chem output averaged over the entire domain between 1700 and 2200 UTC (roughly the times during which OMI is over North America)

In all cases the data points (modeled or measured) used to generate the NO_2 profiles are binned by pressure to generate a profile defined at the same pressures (using pressure as a vertical coordinate) as the scattering weights in the look-up table. Each data point is placed in the bin with the scattering weight pressure closest to the pressure of the data point. When using the DC3-WRF matched profiles (Sect. 2.3), the two greatest surface pressures (1013 and 989) will have essentially no difference, as the matched profiles only extend down to 990 hPa.

3 Results

3.1 Parameter sensitivity study using modeled profiles

We begin by demonstrating the sensitivity of the AMF to modeled lightning NO_x emissions in a general sense. Profiles used in this section are those derived by binning WRF-Chem output from the entire domain for simulations with 0, 500, and 665

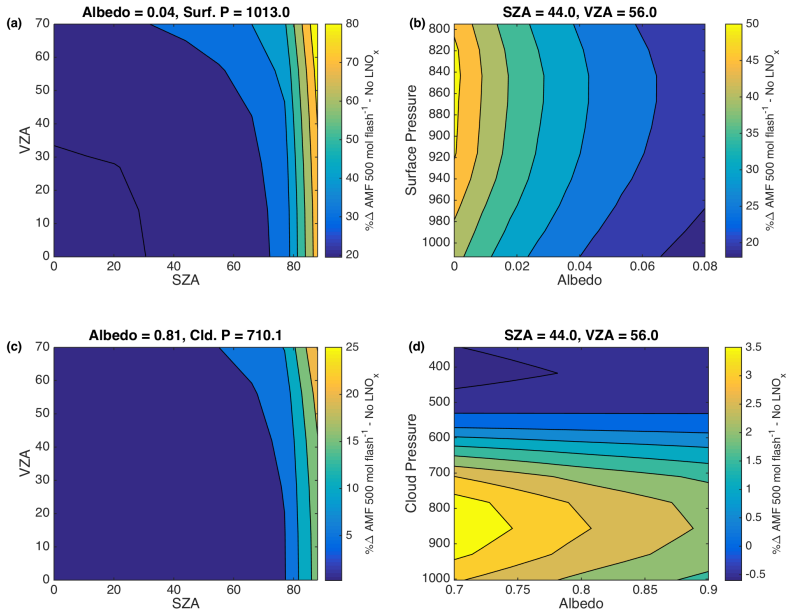

Figure 2. Contour plots of the percent change in the AMF when changing from the mean profile without lightning NO_x to the mean with lightning NO_x (500 mol flash^{-1}), averaged over the whole WRF-Chem domain. The differences are averaged over all values of RAA. In each plot, two parameters are varied while the other two are held constant. The values of the constant parameters are given above each plot. (a) and (b) use a range of albedos and surface pressure representative of clear pixels; (c) and (d) for cloudy pixels.

mol NO flash^{-1} without FDDA nudging (Fig. 1). Figure 2 shows the percent difference in the AMF when using the profile simulated with 500 mol NO flash^{-1} versus 0 mol NO flash^{-1}. In each plot, two of the look-up table inputs are varied and two are held constant. Each plot represents the change averaged over all values of relative azimuth angle (RAA), since RAA has a small impact on the AMF (Fig. S1).

Under both clear and cloudy conditions, the largest differences in AMF between the two profiles are seen at large SZAs (Fig. 2a and c). This reflects the longer average optical path through the upper troposphere (UT) at larger SZAs, causing greater sensitivity to UT NO_2. A similar, though smaller, effect is also seen for larger VZAs.

If viewing geometry is held constant and albedo and surface pressure varied, the largest sensitivity of the AMF to simulated lightning NO_x can be seen at very low albedo and moderate surface pressure ($\sim$ 860 hPa) for clear conditions (Fig 2b). The cause for this is illustrated in Fig. 3; Fig. 3c shows how the scattering weight vectors change with albedo and Fig. 3d shows how they change with surface pressure. Lower albedos yield lower sensitivity to near-surface NO_2 (note that scattering weights are proportional to sensitivity) because a photon that reaches the near-surface NO_2 will likely be absorbed if it scatters into the surface (Hönninger et al., 2004). The 500 mol flash^{-1} profile does have more NO_2 in the boundary layer than the no lightning profile, especially below 900 hPa. This partly balances the increase in UT NO_2 from lightning, as there are increases at both

low and high sensitivity altitudes. As surface pressure decreases (i.e. higher in elevation), the altitude of minimum sensitivity moves up. The surface integration limit for Eq. (1) and (3) reduces as well, removing part of the boundary layer profile. Taken together, these changes put more weight on the UT profile and remove the < 900 hPa increase that counteracts part of the change in the UT (thus increasing the impact of lightning NO_x) until ~ 860 hPa. At ~ 860 hPa, most of the boundary layer is no longer included in the AMF calculation. Figure 1 shows that above ~ 800 hPa, the WRF-Chem profiles start to diverge due to the different amounts of lightning NO_x in each simulation. Therefore, as surface pressure moves above 850–800 hPa, the sensitivity to lightning NO_x begins to decrease because the entire extent of the profile that is integrated changes with changes in the simulated lightning NO_x. Since the profile is normalized to the column amount (Eq. 3), only the relative distribution of NO_2 matters, and the relative distribution changes very little with the magnitude of lightning NO_x emitted when only considering the part of the profile influenced by lightning NO_x.

The effect of changing surface pressure in a regular retrieval will likely be different than that described above, because the above analysis assumes that the profile does not change with surface pressure, where in fact it should, since surface-based emissions will move up with the surface. Consequently, the boundary layer maximum would not be cut off in that case. The effect described here is more consistent with the effect of clouds or an aerosol layer that creates an effectively higher altitude surface (due to scattering), or if using coarse enough a priori profiles that the surface pressure of a pixel is significantly different than the surface pressure in the model used to simulate the profile.

Cloudy conditions exhibit less sensitivity than clear conditions to the amount of lightning NO_x in the modeled profiles due to this shielding effect: in many cases, the cloud is at sufficiently high elevation to obscure the ~~surface~~ part of the NO_2 profile influenced by surface emissions, and therefore restricts the profile to the component influenced by lightning NO_x. As previously discussed with respect to surface pressure, this means that the relative distribution of NO_2 in the visible component of the profile does not change significantly. This is apparent in Fig. 2, where (c) and (d) show responses roughly $\frac{1}{4}$ and $\frac{1}{10}$ times, respectively, compared to (a) and (b).

Cloudy conditions also tend to have more uniform scattering weights (Fig. 4) due in large part to their high albedo. At high albedo, the probability of "losing" photons to absorption at the surface is significantly reduced, so the reduction in sensitivity towards the surface found with low albedos does not occur. At sufficiently high albedos, there is an enhancement in sensitivity near the ~~surface~~ cloud due to the possibility of extended optical paths near the surface from multiple scattering (Richter and Wagner, 2011).

From Fig. 4, it is clear why the impact of lightning NO_x is small in Fig. 2d. For all but the most extreme sun-satellite geometries, the scattering weights are fairly uniform across all altitudes, thus the impact of changes to the relative distribution of NO_2 within the UT is minimized since a UV/visible satellite instrument is similarly sensitive to NO_2 at any altitude under these conditions. At larger SZAs and VZAs, the cloudy scattering weights do decrease towards the ~~surface~~ cloud because Rayleigh scattering has a greater effect on the transmitted light along the longer beam paths, scattering photons at higher altitudes and so reducing the fraction of photons observed by the satellite that penetrate to the cloud (Richter and Wagner, 2011). However, the impact is less than in clear conditions. From Fig. 2c, at the largest SZA and VZA simulated, the difference in AMF between the no lightning and 500 mol flash^{-1} profiles is +20–25%—large, but only one-fourth that of clear conditions.

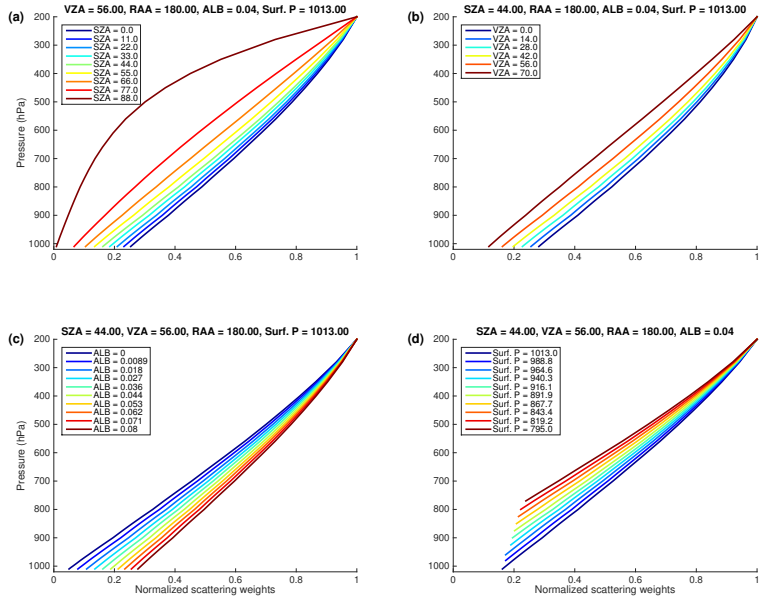

Figure 3. Vectors of scattering weights and their variation with each of the four most important look-up table input parameters. Values are representative of clear-sky conditions. Each scattering weight vector is scaled so that the top most entry is 1. Scattering weights are only shown above the surface pressure.

The difference in the AMF obtained using profiles with 665 and 500 mol NO flash^{-1} follows essentially the same pattern as shown in Figs. 3 and 4, but with $\frac{1}{10}$ to $\frac{1}{5}$ the magnitude (Fig. S2). The only difference in the shape of the contours is that the maximum difference occurs at greater (i.e. lower altitude) surface pressures, because the 665 and 500 mol flash^{-1} profiles are mostly identical in the boundary layer, so the slight countervailing increase in boundary layer NO_2 between the 0 and 500 mol flash^{-1} profiles that offset part of the UT increase is not present.

3.2 Comparison with observed profiles

Given the large sensitivity of AMFs to the presence of lightning NO_x in the a priori profiles, it is necessary to use a priori profiles that are consistent with observations. Figure 5 compares the average NO_2 profile measured in the DC3 campaign (Sect. 2.1) with WRF-Chem profiles averaged along the DC3 flights (Sect. 2.3) for five simulations. It is immediately apparent that the WRF-Chem simulation with no lightning is missing a significant amount of UT NO_2 compared to the observed DC3 profile. Both unnudged WRF-Chem simulations with lightning NO_x enabled do qualitatively capture this UT NO_2; however the vertical distribution is biased compared to the DC3 observations with a maximum at 500 hPa not seen in the observed profile and less NO_2 between 300–200 hPa than in the observed profile.

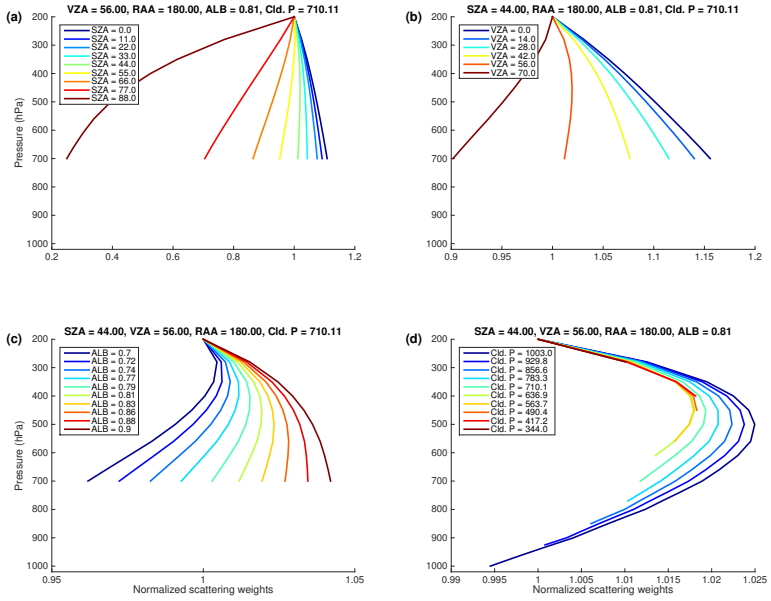

Figure 4. As in Fig. 3, but for cloudy conditions. Note that the x-axis limits are different from Fig. 3 and each other.

We consider how significant these differences between the simulated and observed profiles are in the context of the AMF calculation. To focus only on the effect of the UT profile, we use hybrid profiles. The hybrid profiles for the unnudged 500 mol flash^{-1} are illustrated in Fig. 5b. The free troposphere hybrid uses the DC3 profile up to 750 hPa and the WRF-Chem profile above that, while the mid-troposphere hybrid only uses the WRF-Chem profile between 750 and 375 hPa. The free tropospheric hybrid profile focuses on the effect of lightning NO_2 on the AMF by removing the difference in the boundary layer between the WRF-Chem and DC3 profiles, while the mid-troposphere hybrid similarly focuses on the effect of the local NO_2 maximum around 500 hPa that is not present in the DC3 profile.

Table 2 gives the results of AMF sensitivity tests (Sect. 2.5.2) on various hybrid combinations of the profiles in Fig. 5a. We present the average AMF obtained in the sensitivity test using each hybrid profile, and its percent difference relative to the mean AMF obtained using the DC3 profile. Because OMI experiences a more limited range of solar zenith angles during summer over the US ($\sim 30° \pm 6°$, on average) than are defined in the TOMRAD look-up table, we also compare a subset of the AMF sensitivity tests with the SZA $< 40°$.

Comparing the 0 mol flash^{-1} WRF-Chem profiles to the DC3 profile, we see that difference NO_2 above 375 hPa has a large impact on the AMF, causing a ~~26–35~~25–35% low bias in the AMF, depending on the SZAs considered. Adding lightning NO_x to the WRF-Chem simulation (the 500 and 665 mol flash^{-1} profiles) corrects this bias. Recent work (Nault et al., 2017) suggests that the previous mean value of mol NO flash^{-1} (500 mol flash^{-1}) is 33% low; comparing the AMFs obtained from

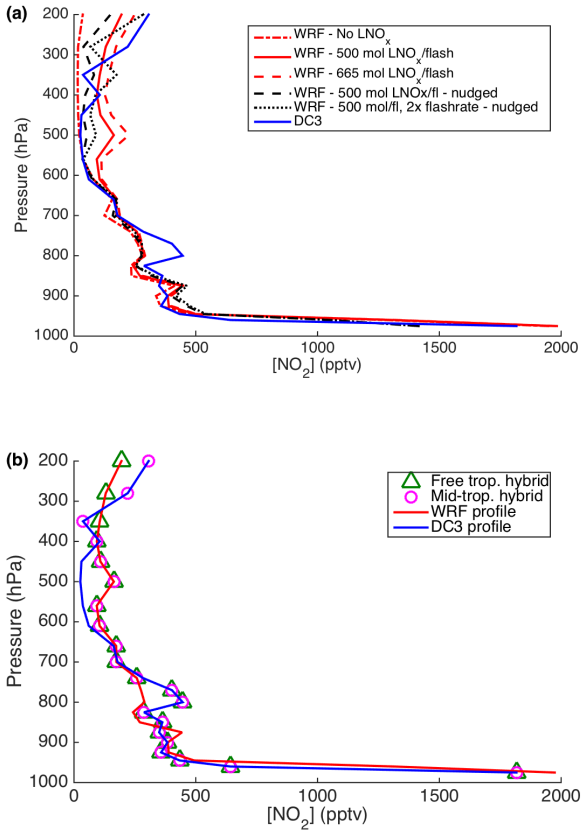

Figure 5. (a) Comparison of the NO_2 profiles obtained from binning all DC3 data and WRF-Chem output along the DC3 flight track (Sect 2.3) to pressure bins centered on the pressure the scattering weights are defined at. (b) The binned DC3 and WRF-Chem (500 mol flash^{-1}, no nudging) profiles; green triangles mark pressure levels from each profiles used in the free troposphere hybrid profile, magenta circles mark pressure levels used in the mid-troposphere hybrid profile.

Profile	Avg. AMF	%Δ AMF vs. DC3	Avg. AMF SZA $< 40°$	%Δ AMF(SZA $< 40°$) vs. DC3
DC3	~~1.56~~ 1.59	–	~~1.30~~ 1.33	–
Free Trop. Hybrid-0	~~1.02~~ 1.04	~~−34.87~~ −34.42	~~0.96~~ 0.99	~~−26.01~~ −25.51
Mid. Trop. Hybrid-0	~~1.55~~ 1.58	~~−0.87~~ −0.80	~~1.29~~ 1.31	~~−1.10~~ −1.02
Free Trop. Hybrid-500	~~1.51~~ 1.54	~~−3.40~~ −3.56	~~1.29~~ 1.31	~~−0.89~~ −1.07
Mid. Trop. Hybrid-500	~~1.60~~ 1.63	~~2.26~~ 2.12	~~1.34~~ 1.36	~~2.86~~ 2.69
Free Trop. Hybrid-665	~~1.62~~ 1.64	~~3.54~~ 3.24	~~1.36~~ 1.39	~~4.70~~ 4.37
Mid. Trop. Hybrid-665	~~1.62~~ 1.64	~~3.44~~ 3.23	~~1.36~~ 1.38	~~4.24~~ 3.98
Free Trop. Hybrid-500, nudge	~~1.26~~ 1.29	~~−19.37~~ −19.18	~~1.12~~ 1.15	~~−13.93~~ −13.73
Mid. Trop. Hybrid-500, nudge	~~1.56~~ 1.59	~~−0.08~~ −0.07	~~1.30~~ 1.33	~~−0.08~~ −0.07
Free Trop. Hybrid-500, nudge, 2x flashrate	~~1.48~~ 1.51	~~−5.45~~ −5.52	~~1.26~~ 1.29	~~−3.05~~ −3.13
Mid. Trop. Hybrid-500, nudge, 2x flashrate	~~1.58~~ 1.61	~~1.18~~ 1.11	~~1.32~~ 1.34	~~1.33~~ 1.26

Table 2. Results of the AMF sensitivity tests on the hybrid profiles in Fig. 5

profiles generated with 500 and 665 mol flash^{-1} changes the sign of the AMF bias relative to the DC3 profile, but not its magnitude.

The purpose of including the mid-troposphere hybrid profiles, which only use the WRF-Chem profile between 700 and 375 hPa, is to evaluate the impact of the simulated NO_2 maximum around 500 hPa. In almost all cases, the bias of these hybrid profiles against the DC3 profile is less than the corresponding free-troposphere hybrid. Thus, that anomalous maximum at 500 hPa has a smaller impact than the overall presence or absence of lightning NO_2, as one would expect.

An additional complication arises when considering the effect of nudging the model meteorology. By default, the meteorology in WRF is driven by the model's internal physics and is constrained by reanalysis meteorology only through the initial and boundary conditions. WRF has the option, however, to constrain meteorology throughout the domain using four dimensional data analysis (FDDA) nudging. Temperature and water vapor mixing ratio can both be nudged, and both are used in the Grell 3D cumulus physics calculation in WRF (Grell, 1993; Grell and Dévényi, 2002), which outputs the cloud top height that is used by the Price and Rind (1992) parameterization of flash rate.

With FDDA nudging, lightning flash rates throughout the domain decreased by approximately a factor of 2 compared to the unnudged case (Fig. S3). Comparing both temperature and water vapor mixing ratios from nudged and unnudged simulations, we find that nudged and unnudged temperature profiles only differ by $\sim$ 1–2 K at each model level on average, and both agree well with DC3 measurements. The water vapor profiles change more significantly, and the profiles resulting from the nudged simulation agree better with those measured during DC3 (Fig. S4). Therefore, we conclude that the changes to the water vapor profiles are responsible for the 2x change in lightning flash rates.

Using the NO_2 profiles resulting from the nudged simulation with 500 mol flash^{-1}, we see in Fig. 5a that there is significantly less simulated NO_2 near 200 hPa than in the unnudged run and the DC3 observations. The AMF sensitivity tests show that this

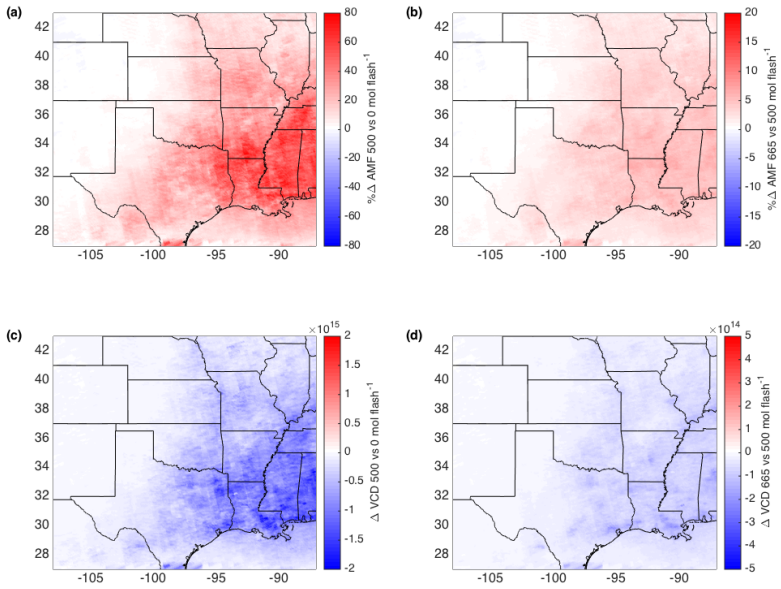

Figure 6. Average percent difference in AMFs (a,b) and absolute difference in VCDs (c,d) averaged over the time period 18 May–23 June 2012. (a,c) Difference between profiles generated using 500 mol NO flash^{-1} and 0 mol NO flash^{-1}; (b,d) Difference between profiles generated using 665 mol NO flash^{-1} and 500 mol NO flash^{-1}. Note that in (c) and (d) the color scale is one-fourth that of (a) and (b).

reintroduces a ~~14–20~~14–19% low bias compared to the AMF derived from the DC3 profile, a significant increase in the bias compared to the unnudged simulation. Doubling the flash rate largely corrects this bias by increasing the NO_2 found in the upper part of the profile (Fig. 5a).

3.3 Effect of varied lightning emissions on BEHR AMFs

To illustrate the impact of missing lightning NO_x on a full retrieval, we use the unnudged WRF-Chem NO_2 profiles simulated with 0, 500 and 665 mol NO flash^{-1} as a priori profiles in the BEHR retrieval and examine the change in both AMF and retrieval NO_2 vertical column density (VCD) with the change in simulated lightning NO_x.

Figure 6 shows the average percent change in AMFs (top) and absolute change in VCDs (bottom) between retrievals using profiles generated using 0 and 500 mol NO flash^{-1} (Fig. 6a, c) and between 500 and 665 mol NO flash^{-1} (Fig. 6b, d). These results were obtained by averaging data from 18 May to 23 June 2012, treating the data as described in Sect. 2.5.1.

Most importantly, we see in Fig. 6a that the change due to the inclusion of lightning NO_2 is not constant throughout the domain, but is regionally specific. The SE US sees the greatest change in AMF, as it has very active lightning (Hudman et al., 2007). This leads to changes in the retrieved VCD of 1 to 2×10^{15} molec. cm^{-2}.

We consider two uncertainty values to determine if this change is significant. Bucsela et al. (2013) calculated a global mean uncertainty of 1×10^{15} molec. cm^{-2} for tropospheric NO_2 VCDs. Boersma et al. (2004) calculated a typical uncertainty of 23% in tropospheric AMFs for polluted conditions. Since, on average, 32 ± 6 (mean $\pm$ 1 σ) pixels contribute to each value in our average, the reduced uncertainty is $\sim 0.2 \times 10^{15}$ molec. cm^{-2} and 4%, respectively. The changes we find in the tropospheric VCD due to the inclusion or exclusion of lightning NO_2 from the a priori profiles exceed that uncertainty in $\sim 50\%$ of the domain; the changes in the AMF exceed the uncertainty in $\sim 70\%$ of the domain.

The effect on the retrieval from increasing the mol NO flash^{-1} from 500 to 665 is about 5–10x smaller, as seen in Fig. 6b, d. In Fig. 1 and Fig. 5, we saw that the change in the UT profile was smaller when increasing the mol flash^{-1} from 500 to 665 compared to increasing from 0 to 500 as expected. The nonlinear nature of the AMF calculation also contributes to the smaller change in AMFs and VCDs between 500 and 665 mol flash^{-1} profiles; as the contribution of lightning NO_2 increases, both the numerator (at the relevant pressure levels) and denominator of Eq. (3) increase. The increasing denominator will cause the same magnitude increase in the numerator to have a smaller effect on the overall AMF.

4 Discussion

Accurately representing lightning NO_2 in a priori profiles for retrieval of NO_2 from space is vital not only when retrieving lightning events, but any retrieval in a region and time period influenced by lightning. ~~While work~~ Work from the DC3 campaign has shown that the lifetime of NO_x in the near field of thunderstorms is remarkably short ($\sim$ 3 h, Nault et al., 2016) due to active chemistry with peroxy radical species convected from the surface~~, once those peroxy radicals are depleted, the UT lifetime of in the far-field from thunderstorms is in the range of 0.5 to 1.5 days (Bertram et al., 2007; Fried et al., 2008; Apel et al., 2012; Nault et al., 201 As shown in Sect. 3.1, this means that the presence or absence of lightning in the a priori profiles has a large effect on the retrieval AMFs in clear-sky conditions which are used to obtain information about boundary layer (e.g. Lamsal et al., 2010; Beirle et al., 20~~

. We note that the WRF-Chem model used here may not be adequately capturing this near-field chemistry as the simulated concentrations of methyl peroxy nitrate (MPN) are significantly lower than those measured by the DC3 campaign, particularly in the range of 300 to 400 hPa. We suspect that modeled concentrations of the methyl peroxy radical precursor are too low, but have not investigated this. However, we do not believe this significantly impacts our conclusions, as when we bin the DC3 MPN data as in Fig. 5, the MPN concentration is $\frac{1}{5}$ to $\frac{1}{10}$ that of NO_x, so the effect on the AMF is expected to be less than the effect of increasing the modeled mol NO flash^{-1} from 500 to 665.

4.1 ~~Effect of nudged meteorology on flash counts~~

~~Additionally,~~ As discussed in Nault et al. (2017) , once those peroxy radicals are depleted, the UT lifetime of NO_x in the far-field from thunderstorms is in the range of 0.5 to 1.5 days (Bertram et al., 2007; Fried et al., 2008; Apel et al., 2012; Nault et al., 2016) . As shown in Sect. 3.1, this means that the presence or absence of lightning NO_2 in the a priori profiles has a large effect on the retrieval AMFs in clear-sky conditions which are used to obtain information about boundary layer NO_x (e.g. Lamsal et al., 2010; Beirle et a

Since many of these studies focus on summer months when thunderstorms are common over the US (Barth et al., 2015) , the results from Sect. 3.2 regarding the reduction in number of lightning flashes when using FDDA nudging towards the NARR reanalysis are particularly relevant, as Laughner et al. (2016) showed the importance of using daily, high-spatial resolution inclusion of lightning NO_2 in the a priori profiles to accurately resolve differences in VCDs upwind and downwind of a city, and suggested the use of nudging to reduce the uncertainty due to wind direction, especially. Our results here indicate that (1) missing is necessary to accurately constrain the emissions. Lightning is less frequent in wintertime, but the southeast US does experience winter lightning (Orville et al., 2001; Hunter et al., 2001) . Therefore, wintertime retrievals will likely see significantly less but nonzero impact from the inclusion of lightning NO_2 in the a priori profileswill lead to large overestimations of VCDs, which, among other things, would lead to overestimates of emissions based on such a retrieval, and (2) that when using nudging within a WRF-Chem simulation to constrain the meteorology, its effect on lightning flash rates must be checked to ensure it does not inadvertently affect the upper tropospheric . Future work will verify this as new a priori profiles are planned for inclusion in the next generation of the BEHR retrieval. These new a priori profiles will correct the absence of modeled lightning NO_2 profilein the BEHR v2.1C a priori profiles.

Nevertheless, although

4.1 Effect of nudged meteorology on flash counts

Although our results showed that the NO_2 profile resulting from the nudged run without doubled flash counts had less UT NO_2 that than the average DC3 profile, we cannot conclude that the flash rates calculated with nudged meteorology are underestimated, particularly as Wong et al. (2013) found the opposite result when comparing to the National Lightning Detection Network. A direct comparison with Wong et al. (2013) is complicated by the different choices of model options (such as cumulus physics: Grell 3D in ours vs. Grell-Devenyi in Wong; Lin vs. Thompson microphysics; NARR vs. NCEP Global Forecasting System Final meteorology). A full analysis of the reason that activating FDDA nudging causes the flash rates to decrease by 50% in our case is beyond the scope of this paper. Empirically, we see that the NO_2 profile generated by the FDDA run with 1x the base flash rate has less UT NO_2 than was observed during DC3 (Fig. 5). Therefore, we cannot say whether this discrepancy in the profile is due to the reduced number of flashes or a too-low average number of moles of NO emitted per flash. Our correction of doubling the nudged flash rate to improve agreement between the modeled and observed profiles was the most straightforward based on the differences between the nudged and unnudged runs.

Laughner et al. (2016) showed the importance of using daily, high-spatial resolution a priori profiles to accurately resolve differences in NO_2 VCDs upwind and downwind of a city, and suggested the use of nudging to reduce the uncertainty due to wind direction, especially. Those results also indicated that using daily, high spatial resolution profiles is essential to directly constrain emissions with satellite observations. Our results here indicate that (1) missing lightning NO_2 in the a priori profiles will lead to large overestimations of VCDs, which, among other things, would lead to overestimates of NO_x emissions based on such a retrieval, and (2) that when using nudging within a WRF-Chem simulation to constrain the meteorology, its effect on lightning flash rates must be checked to ensure it does not inadvertently affect the upper tropospheric NO_2 profile.

4.2 Relevance to cloud slicing

In the context of work using cloud-slicing techniques to derive NO_2 profiles (e.g. Choi et al., 2014), our results suggest that profile shape is a minor contribution to the uncertainty. By using a simulated retrieval with a known NO_2 concentration profile, Choi et al. (2014) estimated 20–30% uncertainty in the NO_2 concentration derived from their cloud-slicing approach. Our work here shows that, for fully cloudy conditions, the change in the AMF between a no lightning and 500 mol flash^{-1} NO_2 profile is $\leqslant 5\%$ (Sect. 3.1)~~; since~~ . Since Choi et al. (2014) used a typical C-shaped NO_2 profile that included lightning NO_2 (e.g. Pickering et al., 1998), based on our results, we expect that any uncertainty should be closer to the difference we observed between the 500 and 665 mol flash^{-1} profiles, $\leqslant 1\%$, although we acknowledge that the analysis in Choi et al. (2014) may include additional sources of uncertainty not captured by our work.

4.3 Relevance to global and geostationary retrievals

To the best of our knowledge, the chemical transport models used to generate the a priori profiles in the NASA Standard Product and KNMI DOMINO product for OMI NO_2 include lightning NO_x in the simulation. However, for researchers wishing to generate high spatial resolution a priori profiles using models such as WRF-Chem or the Community Multiscale Air Quality (CMAQ) model that have thus far focused on lower troposphere chemistry for air quality implications, it is important to verify whether that model setup includes lightning NO_x. Retrievals that use a priori profiles without a lightning NO_x parameterization will suffer from a regionally dependent, systematic positive bias in retrieved VCDs. This is particularly difficult to account for given that the bias is unlikely to be reduced by averaging, nor is it constant enough spatially to be addressed as a coarse, ad hoc correction to the AMF.

The next generation of polar orbiting (TROPOMI) and geostationary (TEMPO, Sentinel-5, GEMS) UV-visible spetrometers will have even greater spatial resolution than OMI. To get the most value out of these high spatial resolution detectors, high spatial and temporal resolution a priori profiles are necessary (e.g. Russell et al., 2011; Laughner et al., 2016; Goldberg et al., 2017). High resolution air quality models, such as WRF-Chem or CMAQ, are one avenue to produce a priori profiles with resolution of 1 to 10 km. Ensuring that lightning NO_x is adequately parameterized in the models is essential for any retrieval, but especially for geostationary satellites such as TEMPO, which will retrieve NO_2 at larger solar zenith angles than polar orbiting satellites. At such large SZAs, the relative importance of accurate UT NO_2 profiles is even greater than for OMI retrievals.

5 Conclusions

We quantify the impact of lightning NO_2 on a priori profiles used in satellite retrievals of NO_2. We find that, on average, compared to an average NO_2 profile constructed from measurements taken during the DC3 campaign, excluding lightning NO_2 leads to a -35% bias in the AMF if all solar zenith angles are considered, and ~~-26%~~ -25% for solar zenith angles relevant to the OMI instrument in the summer. We find that, using the Price and Rind (1992) parameterization in WRF-Chem

with the Grell-3D cumulus model, 500 to 665 mol NO flash^{-1} yields AMFs within ~~5~~$\sim 5\%$ of those obtained using the DC3 profile. We also find that, if FDDA nudging is used, flash rates must be multiplied by a factor of 2 to get the same agreement with this model configuration.

Implementing profiles generated with 0, 500, and 665 mol NO flash^{-1} in the BEHR retrieval, we find that the effect on the AMF is very regionally dependent. ~~Changing~~ For summertime retrievals, changing from profiles using 0 mol NO flash^{-1} to 500 mol NO flash^{-1} shows the largest increase in the AMF of ~~$\sim 80\%$~~ 50–80% occurring in the SE US. This results in changes to the VCD of 1 to 2×10^{15} molec. cm^{-2}. The effect is nearly 0 on the west edge of the domain, over the Rocky Mountains. Further increasing the mol NO flash^{-1} from 500 to 665 only results in a $\sim 5\%$ change to the AMF.

Code and data availability. The AutoWRFChem code used to automate the preparation of meteorological and chemical inputs and execution of WRF-Chem is available at https://github.com/CohenBerkeleyLab/AutoWRFChem-Base (Laughner, 2017b) . The versions of WRF-Chem v3.5.1, WPS v3.5.1, NEI conversion utility, MEGAN biogenic model, and MOZBC utility with the modification to handle the R2SMH chemical mechanism and corresponding emissions are available at https://github.com/CohenBerkeleyLab/AutoWRFChem-R2SMH, v1.0.0. The retrievals used in Section 3.3 are available at https://doi.org/10.6078/D19S9D (Laughner, 2017c) . The analysis code, TOMRAD LUT, and WRF-Chem namelist files are available at https://doi.org/10.5281/zenodo.1001803 (Laughner, 2017a) . For access to the BEHR algorithm contact the corresponding author, R.C. Cohen.

Competing interests. The authors declare no competing interests.

Acknowledgements. The authors gratefully acknowledge support from the NASA ESS Fellowship NNX14AK89H, NASA grant NNX15AE37G, and the TEMPO project grant SV3-83019. The MODIS Aqua L2 Clouds 5-Min Swath 1 and 5km (MYD06_L2) and MODIS Terra+Aqua Albedo 16-Day L3 Global 0.05Deg CMG V005 were acquired from the Level-1 and Atmospheric Archive and Distribution System (LAADS) Distributed Active Archive Center (DAAC), located in the Goddard Space Flight Center in Greenbelt, Maryland (https://ladsweb.nascom.nasa.gov/). We acknowledge use of the WRF-Chem preprocessor tools mozbc, fire_emiss, etc. provided by the Atmospheric Chemistry Observations and Modeling Lab (ACOM) of NCAR. This research used the Savio computational cluster resource provided by the Berkeley Research Computing program at the University of California, Berkeley (supported by the UC Berkeley Chancellor, Vice Chancellor of Research, and Office of the CIO). The authors also wish to thank Mary Barth for assistance with the lightning NO_x module in WRF-Chem.

References

Acarreta, J. R., De Haan, J. F., and Stammes, P.: Cloud pressure retrieval using the O2-O2 absorption band at 477 nm, J. Geophys. Res. Atmos., 109, doi:10.1029/2003JD003915, http://dx.doi.org/10.1029/2003JD003915, d05204, 2004.

Allen, D. J., Pickering, K. E., Pinder, R. W., Henderson, B. H., Appel, K. W., and Prados, A.: Impact of lightning-NO on eastern United States photochemistry during the summer of 2006 as determined using the CMAQ model, Atmos. Chem. Phys., 12, 1737–1758, doi:10.5194/acp-12-1737-2012, 2012.

Apel, E. C., Olson, J. R., Crawford, J. H., Hornbrook, R. S., Hills, A. J., Cantrell, C. A., Emmons, L. K., Knapp, D. J., Hall, S., Mauldin III, R. L., Weinheimer, A. J., Fried, A., Blake, D. R., Crounse, J. D., Clair, J. M. S., Wennberg, P. O., Diskin, G. S., Fuelberg, H. E., Wisthaler, A., Mikoviny, T., Brune, W., and Riemer, D. D.: Impact of the deep convection of isoprene and other reactive trace species on radicals and ozone in the upper troposphere, Atmos. Chem. Phys., 12, 1135–1150, doi:10.5194/acp-12-1135-2012, http://www.atmos-chem-phys.net/12/1135/2012/, 2012.

Barth, M. C., Cantrell, C. A., Brune, W. H., Rutledge, S. A., Crawford, J. H., Huntrieser, H., Carey, L. D., MacGorman, D., Weisman, M., Pickering, K. E., Bruning, E., Anderson, B., Apel, E., Biggerstaff, M., Campos, T., Campuzano-Jost, P., Cohen, R., Crounse, J., Day, D. A., Diskin, G., Flocke, F., Fried, A., Garland, C., Heikes, B., Honomichl, S., Hornbrook, R., Huey, L. G., Jimenez, J. L., Lang, T., Lichtenstern, M., Mikoviny, T., Nault, B., O'Sullivan, D., Pan, L. L., Peischl, J., Pollack, I., Richter, D., Riemer, D., Ryerson, T., Schlager, H., Clair, J. S., Walega, J., Weibring, P., Weinheimer, A., Wennberg, P., Wisthaler, A., Wooldridge, P. J., and Ziegler, C.: The Deep Convective Clouds and Chemistry (DC3) Field Campaign, Bull. Am. Met. Soc., 96, 1281–1309, doi:10.1175/bams-d-13-00290.1, 2015.

Beirle, S., Salzmann, M., Lawrence, M. G., and Wagner, T.: Sensitivity of satellite observations for freshly produced lightning NO_x, Atmospheric Chemistry and Physics, 9, 1077–1094, doi:10.5194/acp-9-1077-2009, http://www.atmos-chem-phys.net/9/1077/2009/, 2009.

Beirle, S., Boersma, K., Platt, U., Lawrence, M., and Wagner, T.: "Megacity Emissions and Lifetimes of Nitrogen Oxides Probed from Space", Science, 333, 1737–1739, 2011.

Bertram, T. H., Perring, A. E., Wooldridge, P. J., Crounse, J. D., Kwan, A. J., Wennberg, P. O., Scheuer, E., Dibb, J., Avery, M., Sachse, G., Vay, S. A., Crawford, J. H., McNaughton, C. S., Clarke, A., Pickering, K. E., Fuelberg, H., Huey, G., Blake, D. R., Singh, H. B., Hall, S. R., Shetter, R. E., Fried, A., Heikes, B. G., and Cohen, R. C.: Direct Measurements of the Convective Recycling of the Upper Troposphere, Science, 315, 816–820, doi:10.1126/science.1134548, 2007.

Boccippio, D., Cummins, K., Christian, H., and Goodman, S.: Combined Satellite- and Surface-Based Estimation of the Intracloud–Cloud-to-Ground Lightning Ratio over the Continental United States, Mon. Weather Rev., 129, 108–122, 2001.

Boersma, K., Bucsela, E., Brinksma, E., and Gleason, J.: NO_2, in: OMI Algorithm Theoretical Basis Document, vol 4, OMI Trace Gas Algorithms, ATB-OMI-04, version 2.0, pp. 13–36, http://eospso.nasa.gov/sites/default/files/atbd/ATBD-OMI-04.pdf, 2002.

Boersma, K., Eskes, H., and Brinksma, E.: "Error analysis for tropospheric NO_2 retrieval from space, J. Geophys. Res. Atmos., 106, D04 311, doi:10.1029/2003JD003962, 2004.

Boersma, K., Eskes, H., Dirksen, R., van der A, R., Veefkind, J., Stammes, P., Huijnen, V., Kleipool, Q., Sneep, M., Claas, J., Leitão, J., Richter, A., Zhou, Y., and Brunner, D.: "An improved tropospheric NO_2 column retrieval algorithm for the Ozone Monitoring Instrument, Atmos. Meas. Tech., 4, 1905–1928, doi:10.5194/amt-4-1905-2011, 2011.

Browne, E. C., Perring, A. E., Wooldridge, P. J., Apel, E., Hall, S. R., Huey, L. G., Mao, J., Spencer, K. M., Clair, J. M. S., Weinheimer, A. J., Wisthaler, A., and Cohen, R. C.: Global and regional effects of the photochemistry of $CH_3O_2NO_2$: evidence from ARCTAS, Atmospheric Chemistry and Physics, 11, 4209–4219, doi:10.5194/acp-11-4209-2011, https://www.atmos-chem-phys.net/11/4209/2011/, 2011.

Browne, E. C., Wooldridge, P. J., Min, K.-E., and Cohen, R. C.: On the role of monoterpene chemistry in the remote continental boundary layer, Atmos. Chem. Phys., 14, 1225–1238, doi:10.5194/acp-14-1225-2014, 2014.

Bucsela, E., Krotkov, N., Celarier, E., Lamsal, L., Swartz, W., Bhartia, P., Boersma, K., Veefkind, J., Gleason, J., and Pickering, K.: "A new tropospheric and stratospheric NO_2 retrieval algorithm for nadir-viewing satellite instruments: applications to OMI, Atmos. Meas. Tech., 6, 2607–2626, doi:10.5194/amt-6-2607-2013, 2013.

Bucsela, E. J., Celarier, E. A., Wenig, M. O., Gleason, J. F., Veefkind, J. P., Boersma, K. F., and Brinksma, E. J.: Algorithm for NO_2 vertical column retrieval from the ozone monitoring instrument, IEEE T. Geosci. Remote, 44, 1245–1258, doi:10.1109/TGRS.2005.863715, 2006.

Choi, S., Joiner, J., Choi, Y., Duncan, B. N., Vasilkov, A., Krotkov, N., and Bucsela, E.: First estimates of global free-tropospheric NO_2 abundances derived using a cloud-slicing technique applied to satellite observations from the Aura Ozone Monitoring Instrument (OMI), Atmos. Chem. Phys., 14, 10 565–10 588, doi:10.5194/acp-14-10565-2014, http://www.atmos-chem-phys.net/14/10565/2014/, 2014.

Cooray, V., Rahman, M., and Rakov, V.: On the NOx production by laboratory electrical discharges and lightning, J. Atmos. Sol. Terr. Phys., 71, 1877–1889, doi:10.1016/j.jastp.2009.07.009, 2009.

Emmons, L. K., Walters, S., Hess, P. G., Lamarque, J.-F., Pfister, G. G., Fillmore, D., Granier, C., Guenther, A., Kinnison, D., Laepple, T., Orlando, J., Tie, X., Tyndall, G., Wiedinmyer, C., Baughcum, S. L., and Kloster, S.: Description and evaluation of the Model for Ozone and Related chemical Tracers, version 4 (MOZART-4), Geosci. Model Dev., 3, 43–67, doi:10.5194/gmd-3-43-2010, http://www.geosci-model-dev.net/3/43/2010/, 2010.

EPA: Air Pollutant Emissions Trends Data, https://www.epa.gov/air-emissions-inventories/air-pollutant-emissions-trends-data, 2016.

Fried, A., Olson, J. R., Walega, J. G., Crawford, J. H., Chen, G., Weibring, P., Richter, D., Roller, C., Tittel, F., Porter, M., Fuelberg, H., Halland, J., Bertram, T. H., Cohen, R. C., Pickering, K., Heikes, B. G., Snow, J. A., Shen, H., O'Sullivan, D. W., Brune, W. H., Ren, X., Blake, D. R., Blake, N., Sachse, G., Diskin, G. S., Podolske, J., Vay, S. A., Shetter, R. E., Hall, S. R., Anderson, B. E., Thornhill, L., Clarke, A. D., McNaughton, C. S., Singh, H. B., Avery, M. A., Huey, G., Kim, S., and Millet, D. B.: Role of convection in redistributing formaldehyde to the upper troposphere over North America and the North Atlantic during the summer 2004 INTEX campaign, J. Geophys. Res. Atmos., 113, D17 306, doi:10.1029/2007JD009760, 2008.

Goldberg, D. L., Lamsal, L. N., Loughner, C. P., Swartz, W. H., Lu, Z., and Streets, D. G.: A high-resolution and observationally constrained OMI NO_2 satellite retrieval, Atmos. Chem. Phys., 17, 11 403–11 421, doi:10.5194/acp-17-11403-2017, https://www.atmos-chem-phys.net/17/11403/2017/, 2017.

Goliff, W. S., Stockwell, W. R., and Lawson, C. V.: The regional atmospheric chemistry mechanism, version 2, Atmos. Environ., 68, 174 – 185, doi:10.1016/j.atmosenv.2012.11.038, 2013.

Grell, G. A.: Prognostic Evaluation of Assumptions Used by Cumulus Parameterizations, Mon. Weather Rev., 121, 764–787, doi:10.1175/1520-0493(1993)121<0764:PEOAUB>2.0.CO;2, 1993.

Grell, G. A. and Dévényi, D.: A generalized approach to parameterizing convection combining ensemble and data assimilation techniques, Geophys. Res. Lett., 29, 38–1–38–4, doi:10.1029/2002gl015311, 2002.

Grell, G. A., Peckham, S. E., Schmitz, R., McKeen, S. A., Frost, G., Skamarock, W. C., and Eder, B.: Fully coupled "online" chemistry within the {WRF} model, Atmos. Environ., 39, 6957 – 6975, doi:10.1016/j.atmosenv.2005.04.027, 2005.

Guenther, A., Karl, T., Harley, P., Wiedinmyer, C., Palmer, P. I., and Geron, C.: Estimates of global terrestrial isoprene emissions using MEGAN (Model of Emissions of Gases and Aerosols from Nature), Atmos. Chem. Phys., 6, 3181–3210, doi:10.5194/acp-6-3181-2006, http://www.atmos-chem-phys.net/6/3181/2006/, 2006.

Hastings, D. and Dunbar, P.: Global Land One-kilometer Base Elevation (GLOBE) Digital Elevation Model, Documentation, Volume 1.0. National Oceanic and Atmospheric Administration, National Geophysical Data Center, 325 Broadway, Boulder, Colorado 80303, U.S.A., 1999.

Hönninger, G., von Friedeburg, C., and Platt, U.: Multi axis differential optical absorption spectroscopy (MAX-DOAS), Atmospheric Chemistry and Physics, 4, 231–254, doi:10.5194/acp-4-231-2004, http://www.atmos-chem-phys.net/4/231/2004/, 2004.

Hudman, R. C., Jacob, D. J., Turquety, S., Leibensperger, E. M., Murray, L. T., Wu, S., Gilliland, A. B., Avery, M., Bertram, T. H., Brune, W., Cohen, R. C., Dibb, J. E., Flocke, F. M., Fried, A., Holloway, J., Neuman, J. A., Orville, R., Perring, A., Ren, X., Sachse, G. W., Singh, H. B., Swanson, A., and Wooldridge, P. J.: Surface and lightning sources of nitrogen oxides over the United States: Magnitudes, chemical evolution, and outflow, J. Geophys. Res. Atmos., 112, doi:10.1029/2006JD007912, 2007.

Hudman, R. C., Moore, N. E., Mebust, A. K., Martin, R. V., Russell, A. R., Valin, L. C., and Cohen, R. C.: Steps towards a mechanistic model of global soil nitric oxide emissions: implementation and space based-constraints, Atmos. Chem. Phys., 12, 7779–7795, doi:10.5194/acp-12-7779-2012, http://www.atmos-chem-phys.net/12/7779/2012/, 2012.

Hudson, R., Kim, J.-H., and Anne M., T.: On the derivation of tropospheric column ozone from radiances measured by the total ozone mapping spectrometer, J. Geophys. Res. Atmos., 100, 11,134–11,145, 1995.

Hunter, S. M., Underwood, S. J., Holle, R. L., and Mote, T. L.: Winter Lightning and Heavy Frozen Precipitation in the Southeast United States, Weather Forecasting, 16, 478–490, doi:10.1175/1520-0434(2001)016<0478:wlahfp>2.0.co;2, https://doi.org/10.1175/1520-0434(2001)016<0478:wlahfp>2.0.co;2, 2001.

Jaeglé, L., Jacob, D. J., Wang, Y., Weinheimer, A. J., Ridley, B. A., Campos, T. L., Sachse, G. W., and Hagen, D. E.: Sources and chemistry of NOx in the upper troposphere over the United States, Geophys. Res. Lett., 25, 1705–1708, doi:10.1029/97GL03591, 1998.

Krotkov, N. A., Lamsal, L. N., Celarier, E. A., Swartz, W. H., Marchenko, S. V., Bucsela, E. J., Chan, K. L., Wenig, M., and Zara, M.: The version 3 OMI NO_2 standard product, Atmos. Meas. Tech., 10, 3133–3149, doi:10.5194/amt-10-3133-2017, https://www.atmos-meas-tech.net/10/3133/2017/, 2017.

Kuhlmann, G., Lam, Y. F., Cheung, H. M., Hartl, A., Fung, J. C. H., Chan, P. W., and Wenig, M. O.: Development of a custom OMI NO_2 data product for evaluating biases in a regional chemistry transport model, Atmos. Chem. Phys., 15, 5627–5644, doi:10.5194/acp-15-5627-2015, 2015.

Lamsal, L. N., Martin, R. V., van Donkelaar, A., Celarier, E. A., Bucsela, E. J., Boersma, K. F., Dirksen, R., Luo, C., and Wang, Y.: Indirect validation of tropospheric nitrogen dioxide retrieved from the OMI satellite instrument: Insight into the seasonal variation of nitrogen oxides at northern midlatitudes, J. Geophys. Res. Atmos., 115, doi:10.1029/2009JD013351, 2010.

Lamsal, L. N., Duncan, B. N., Yoshida, Y., Krotkov, N. A., Pickering, K. E., Streets, D. G., and Lu, Z.: U.S. NO_2 trends (2005–2013): EPA Air Quality System (AQS) data versus improved observations from the Ozone Monitoring Instrument (OMI), Atmos. Environ., 110, 130–143, doi:10.1016/j.atmosenv.2015.03.055, 2015.

Laughner, J. L.: Analysis code and intermediate data for "Quantification of the effect of modeled lightning NO_2 on UV-visible air mass factors", doi:10.5281/zenodo.1001803, 2017a.

Laughner, J. L.: AutoWRFChem-Base v0.1.0: Automation for the WRF-Chem model, doi:10.5281/zenodo.834798, 2017b.

Laughner, J. L.: Demonstration retrievals from "Quantification of the effect of modeled lightning NO_2 on UV-visible air mass factors", doi:10.6078/D19S9D, 2017c.

Laughner, J. L., Zare, A., and Cohen, R. C.: Effects of daily meteorology on the interpretation of space-based remote sensing of NO_2, Atmospheric Chemistry and Physics, 16, 15 247–15 264, doi:10.5194/acp-16-15247-2016, http://www.atmos-chem-phys.net/16/15247/2016/, 2016.

Levelt, P., van der Oord, G., Dobber, M., Mälkki, A., Visser, H., de Vries, J., Stammes, P., Lundell, J., and Saari, H.: The Ozone Monitoring Instrument, IEEE Trans. Geosci. Remote Sense., 44, 1093–1101, doi:10.1109/TGRS.2006.872333, 2006.

Lin, J.-T., Liu, M.-Y., Xin, J.-Y., Boersma, K. F., Spurr, R., Martin, R., and Zhang, Q.: Influence of aerosols and surface reflectance on satellite NO_2 retrieval: seasonal and spatial characteristics and implications for NO_x emission constraints, Atmos. Chem. Phys., 15, 11 217–11 241, doi:10.5194/acp-15-11217-2015, 2015.

Lin, Y.-L., Farley, R. D., and Orville, H. D.: Bulk Parameterization of the Snow Field in a Cloud Model, J. Clim. Appl. Meteorol., 22, 1065–1092, 1983.

Liu, F., Beirle, S., Zhang, Q., Dörner, S., He, K., and Wagner, T.: NOx lifetimes and emissions of cities and power plants in polluted background estimated by satellite observations, Atmos. Chem. Phys., 16, 5283–5298, doi:10.5194/acp-16-5283-2016, 2016.

Liu, F., Beirle, S., Zhang, Q., van der A, R. J., Zheng, B., Tong, D., and He, K.: NO_x emission trends over Chinese cities estimated from OMI observations during 2005 to 2015, Atmos. Chem. Phys. Discuss., pp. 1–21, doi:10.5194/acp-2017-369, 2017.

Liu, Y., Bourgeois, A., Warner, T., Swerdlin, S., and Hacker, J.: Implementation of the observation-nudging based on FDDA into WRF for supporting AFEC test operations. 6th WRF Conference, NCAR, Boulder, CO, USA, 2006.

Lu, Z., Streets, D., de Foy, B., Lamsal, L., Duncan, B., and Xing, J.: "Emissions of nitrogen oxides from US urban areas: estimation from Ozone Monitoring Instrument retrievals for 2005–2014", Atmos. Chem. Phys., 15, 10 367–10 383, doi:10.5194/acp-15-10367-2015, 2015.

Martin, R., Sauvage, B., Folkins, I., Sioris, C., Boone, C., Bernath, P., and Ziemke, J.: Space-based constraints on the production of nitric oxide by lightning, J. Geophys. Res. Atmos., 112, doi:10.1029/2006JD007831, 2007.

McLinden, C. A., Fioletov, V., Boersma, K. F., Kharol, S. K., Krotkov, N., Lamsal, L., Makar, P. A., Martin, R. V., Veefkind, J. P., and Yang, K.: Improved satellite retrievals of NO_2 and SO_2 over the Canadian oil sands and comparisons with surface measurements, Atmos. Chem. Phys., 14, 3637–3656, doi:10.5194/acp-14-3637-2014, 2014.

Mebust, A. and Cohen, R.: Observations of a seasonal cycle in NO_x emissions from fires in African woody savannas, Geophys. Res. Lett., 40, 1451–1455, doi:10.1002/grl.50343, 2013.

Mebust, A. and Cohen, R.: Space-based observations of fire NO_x emissions coefficients: a global biome-scale comparison, Atmos. Chem. Phys., 14, 2509–2524, doi:10.5194/acp-14-2509-2014, 2014.

Mebust, A. K., Russell, A. R., Hudman, R. C., Valin, L. C., and Cohen, R. C.: Characterization of wildfire NO_x emissions using MODIS fire radiative power and OMI tropospheric NO_2 columns, Atmos. Chem. Phys., 11, 5839–5851, doi:10.5194/acp-11-5839-2011, 2011.

Miyazaki, K., Eskes, H., and Sudo, K.: Global NO_x emissions estimates derived from an assimilation of OMI tropospheric NO_2 columns, Atmos. Chem. Phys., 12, 2263–2288, doi:10.5194/acp-12-2263-2012, 2012.

Miyazaki, K., Eskes, H., Sudo, K., and Zhang, C.: Global lightning NO_x production estimated by an assimilation of multiple satellite data sets, Atmos. Chem. Phys., 14, 3277–3305, doi:10.5194/acp-14-3277-2014, 2014.

Nault, B. A., Garland, C., Pusede, S. E., Wooldridge, P. J., Ullmann, K., Hall, S. R., and Cohen, R. C.: Measurements of $CH_3O_2NO_2$ in the upper troposphere, Atmos. Meas. Tech., 8, 987–997, doi:10.5194/amt-8-987-2015, 2015.

Nault, B. A., Garland, C., Wooldridge, P. J., Brune, W. H., Campuzano-Jost, P., Crounse, J. D., Day, D. A., Dibb, J., Hall, S. R., Huey, L. G., Jimenez, J. L., Liu, X., Mao, J., Mikoviny, T., Peischl, J., Pollack, I. B., Ren, X., Ryerson, T. B., Scheuer, E., Ullmann, K., Wennberg,

P. O., Wisthaler, A., Zhang, L., and Cohen, R. C.: Observational Constraints on the Oxidation of NOx in the Upper Troposphere, J. Phys. Chem. A, 120, 1468–1478, doi:10.1021/acs.jpca.5b07824, 2016.

Nault, B. A., Laughner, J. L., Wooldridge, P. J., Crounse, J. D., Dibb, J., Diskin, G., Peischl, J., Podolske, J. R., Pollack, I. B., Ryerson, T. B., Scheuer, E., Wennberg, P. O., and Cohen, R. C.: Lightning NO_x Emissions: Reconciling Measured and Modeled Estimates With Updated NO_x Chemistry, Geophys. Res. Lett., doi:10.1002/2017GL074436, 2017.

Orville, R. E., Huffines, G., Nielsen-Gammon, J., Zhang, R., Ely, B., Steiger, S., Phillips, S., Allen, S., and Read, W.: Enhancement of cloud-to-ground lightning over Houston, Texas, Geophys. Res. Lett., 28, 2597–2600, doi:10.1029/2001GL012990, http://dx.doi.org/10.1029/2001GL012990, 2001.

Ott, L. E., Pickering, K. E., Stenchikov, G. L., Allen, D. J., DeCaria, A. J., Ridley, B., Lin, R.-F., Lang, S., and Tao, W.-K.: Production of lightning NOxand its vertical distribution calculated from three-dimensional cloud-scale chemical transport model simulations, J. Geophys. Res., 115, doi:10.1029/2009jd011880, 2010.

Palmer, P., Jacob, D., Chance, K., Martin, R., Spurr, R., Kurosu, T., Bey, I., Yantosca, R., Fiore, A., and Li, Q.: "Air mass factor formulation for spectroscopic measurements from satellites: Applications to formaldehyde retrievals from the Global Ozone Monitoring Experiment", J. Geophys. Res. Atmos., 106, 14 539–14 550, 2001.

Pickering, K. E., Wang, Y., Tao, W.-K., Price, C., and Müller, J.-F.: J. Geophys. Res., 103, 31 203–31 216, 1998.

Pickering, K. E., Bucsela, E., Allen, D., Ring, A., Holzworth, R., and Krotkov, N.: Estimates of lightning NOx production based on OMI NO2 observations over the Gulf of Mexico, Journal of Geophysical Research: Atmospheres, 121, 8668–8691, doi:10.1002/2015JD024179, http://dx.doi.org/10.1002/2015JD024179, 2015JD024179, 2016.

Price, C. and Rind, D.: A simple lightning parameterization for calculating global lightning distributions, J. Geophys. Res. Atmos., 97, 9919–9933, doi:10.1029/92JD00719, 1992.

Richter, A. and Wagner, T.: The Use of UV, Visible and Near IR Solar Back Scattered Radiation to Determine Trace Gases, in: The Remote Sensing of Tropospheric Composition from Space, edited by Burrows, J., Platt, U., and Borrell, P., Springer, New York, 2011.

Russell, A., Perring, A., Valin, L., Bucsela, E., Browne, E., Min, K., Wooldridge, P., and Cohen, R.: "A high spatial resolution retrieval of NO_2 column densities from OMI: method and evalutation", Atmos. Chem. Phys., 11, 8543–8554, doi:10.5194/acp-11-8543-2011, 2011.

Russell, A. R., Valin, L. C., and Cohen, R. C.: Trends in OMI NO_2 observations over the United States: effects of emission control technology and the economic recession, Atmos. Chem. Phys., 12, 12 197–12 209, doi:10.5194/acp-12-12197-2012, 2012.

Schaaf, C. and Wang, Z.: MCD43C3 MODIS/Terra+Aqua BRDF/Albedo Albedo Daily L3 Global 0.05Deg CMG V006, NASA EOSDIS Land Processes DAAC, doi:10.5067/MODIS/MCD43C3.006, 2015.

Schumann, U. and Huntrieser, H.: The global lightning-induced nitrogen oxides source, Atmos. Chem. Phys., 7, 3823–3907, 2007.

Schwantes, R. H., Teng, A. P., Nguyen, T. B., Coggon, M. M., Crounse, J. D., St. Clair, J. M., Zhang, X., Schilling, K. A., Seinfeld, J. H., and Wennberg, P. O.: Isoprene NO_3 Oxidation Products from the RO_2 + HO_2 Pathway, J. Phys. Chem. A, 119, 10 158–10 171, doi:10.1021/acs.jpca.5b06355, 2015.

Seltzer, K. M., Vizuete, W., and Henderson, B. H.: Evaluation of updated nitric acid chemistry on ozone precursors and radiative effects, Atmos. Chem. Phys., 15, 5973–5986, doi:10.5194/acp-15-5973-2015, 2015.

Sneep, M., de Haan, J. F., Stammes, P., Wang, P., Vanbauce, C., Joiner, J., Vasilkov, A. P., and Levelt, P. F.: Three-way comparison between OMI and PARASOL cloud pressure products, J. Geophys. Res. Atmos., 113, doi:10.1029/2007JD008694, d15S23, 2008.

Stammes, P., Sneep, M., de Haan, J. F., Veefkind, J. P., Wang, P., and Levelt, P. F.: Effective cloud fractions from the Ozone Monitoring Instrument: Theoretical framework and validation, J. Geophys. Res. Atmos., 113, n/a–n/a, doi:10.1029/2007JD008820, 10.1029/2007JD008820, d16S38, 2008.

Thornton, J. A., Wooldridge, P. J., and Cohen, R. C.: Atmospheric NO_2: In Situ Laser-Induced Fluorescence Detection at Parts per Trillion Mixing Ratios, Anal. Chem., 72, 528–539, doi:10.1021/ac9908905, 2000.

Travis, K. R., Jacob, D. J., Fisher, J. A., Kim, P. S., Marais, E. A., Zhu, L., Yu, K., Miller, C. C., Yantosca, R. M., Sulprizio, M. P., Thompson, A. M., Wennberg, P. O., Crounse, J. D., St. Clair, J. M., Cohen, R. C., Laughner, J. L., Dibb, J. E., Hall, S. R., Ullmann, K., Wolfe, G. M., Pollack, I. B., Peischl, J., Neuman, J. A., and Zhou, X.: Why do models overestimate surface ozone in the Southeast United States?, Atmos. Chem. Phys., 16, 13 561–13 577, doi:10.5194/acp-16-13561-2016, https://www.atmos-chem-phys.net/16/13561/2016/, 2016.

Valin, L., Russell, A., and Cohen, R.: "Variations of OH radical in an urban plume inferred from NO_2 column measurements", Geophys. Res. Lett., 40, 1856–1860, doi:10.1002/grl.50267, 2013.

Vinken, G. C. M., Boersma, K. F., van Donkelaar, A., and Zhang, L.: Constraints on ship NO_x emissions in Europe using GEOS-Chem and OMI satellite NO_2 observations, Atmos. Chem. Phys., 14, 1353–1369, doi:10.5194/acp-14-1353-2014, http://www.atmos-chem-phys.net/14/1353/2014/, 2014.

Wong, J., Barth, M. C., and Noone, D.: Evaluating a lightning parameterization based on cloud-top height for mesoscale numerical model simulations, Geosci. Model Dev., 6, 429–443, doi:10.5194/gmd-6-429-2013, 2013.

Zörner, J., Penning de Vries, M., Beirle, S., Sihler, H., Veres, P. R., Williams, J., and Wagner, T.: Multi-satellite sensor study on precipitation-induced emission pulses of NO_x from soils in semi-arid ecosystems, Atmos. Chem. Phys., 16, 9457–9487, doi:10.5194/acp-16-9457-2016, 2016.

Supplemental material to: "Quantification of the effect of modeled lightning NO_2 on UV-visible air mass factors"

Joshua L. Laughner and Ronald C. Cohen

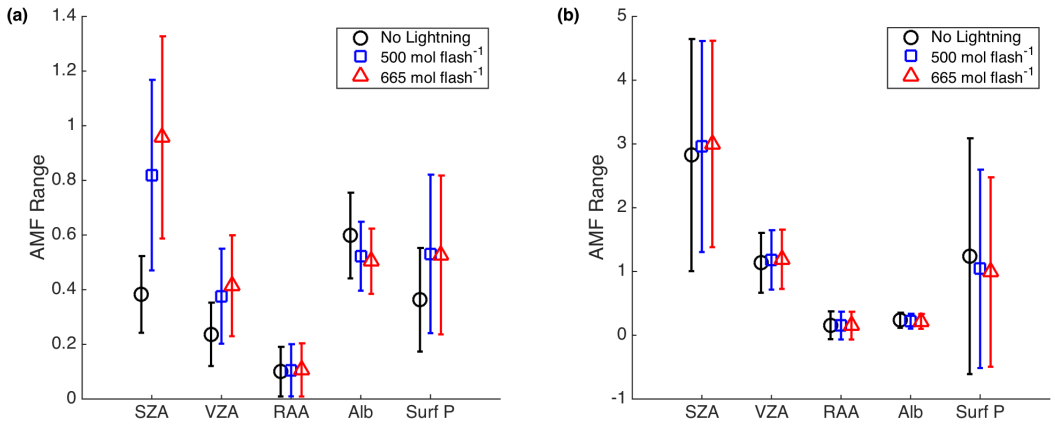

Figure S1: The sensitivity of the AMF to different input parameters to the TOMRAD lookup table for conditions relevant to clear sky pixels (a) and cloudy pixels (b) using the WRF-Chem profile averaged over the entire domain. The marker (circle, square, or triangle) represents the average range of the AMF (max − min) due to varying a given parameter while holding the other four constant; the error bars represent the 1σ variability in that range for all combinations of the other four parameters.

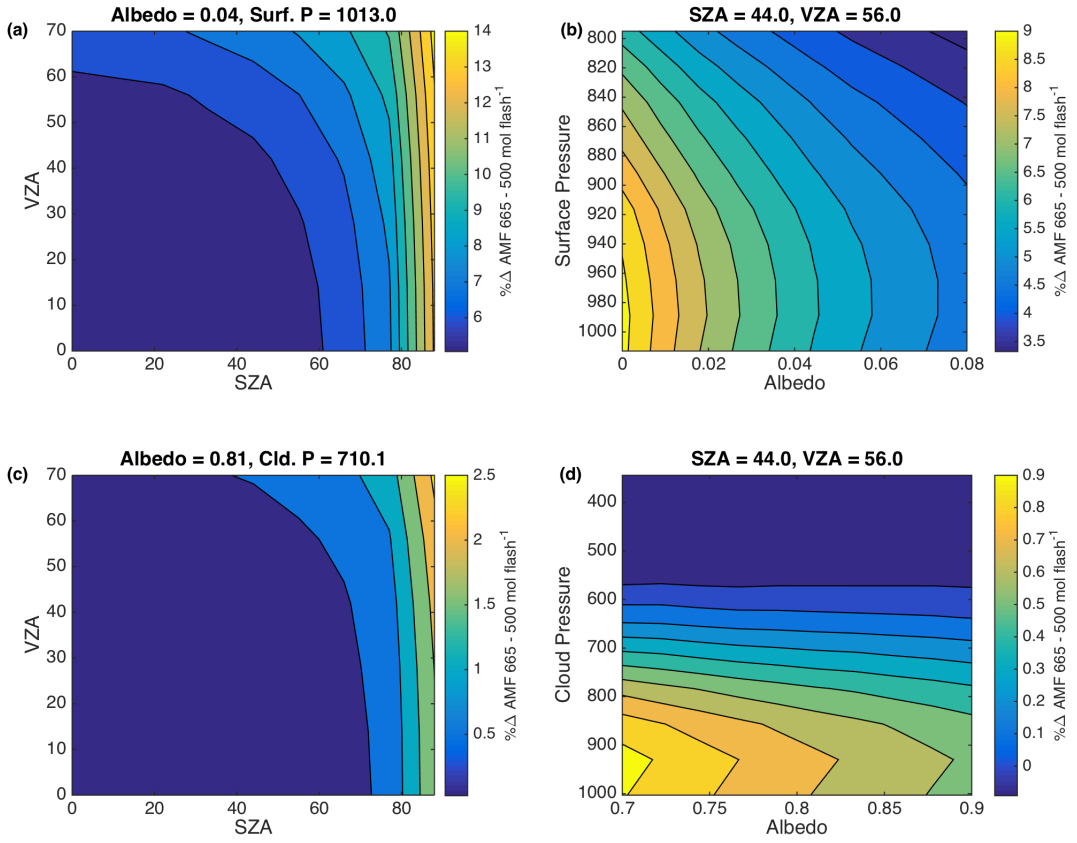

Figure S2: As in Fig. 3 and 4, but now the percent difference in AMF between using profiles generated with 665 and 500 mol NO flash^{-1}.

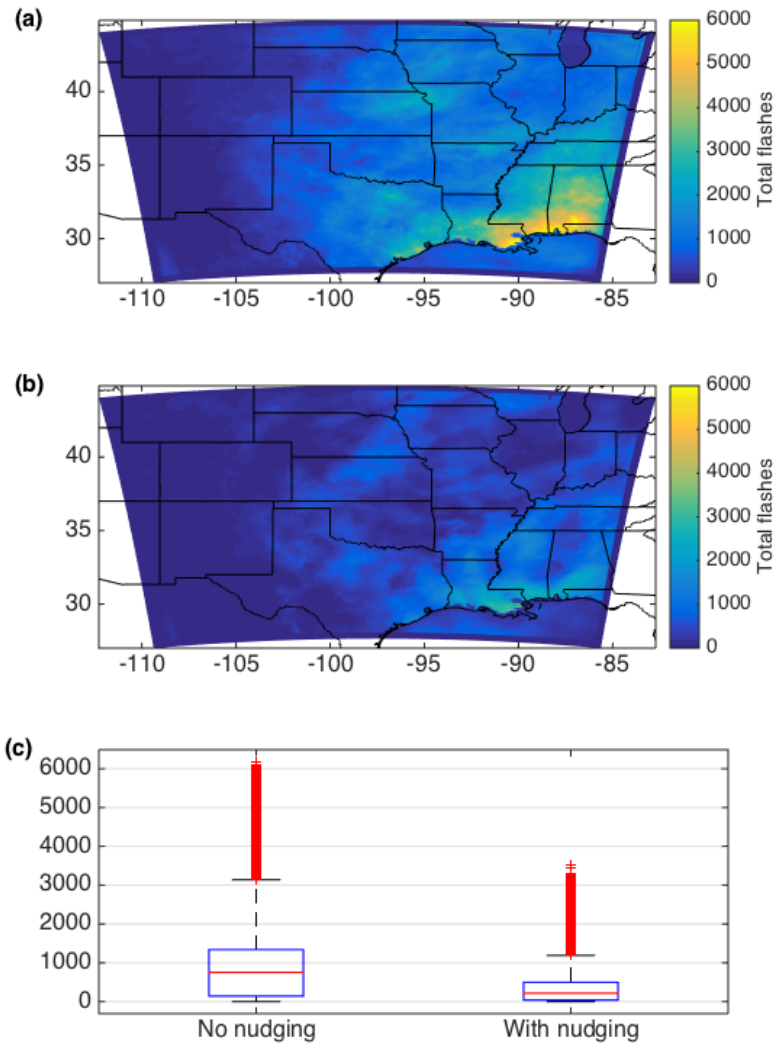

Figure S3: The effect of FDDA nudging on number of lightning flashes. (a) Total number of modeled lightning flashes during the entire modeled time period (13 May to 24 June 2012) without nudging. (b) Same as (a), but for the model run with nudging. (c) Box plot of the statistics for total number of modeled flashes across the domain. The central mark is the median, the box edges the upper and lower quartiles, the ends of the whiskers are the greatest and least non-outlier value, and the individual marks are outliers.

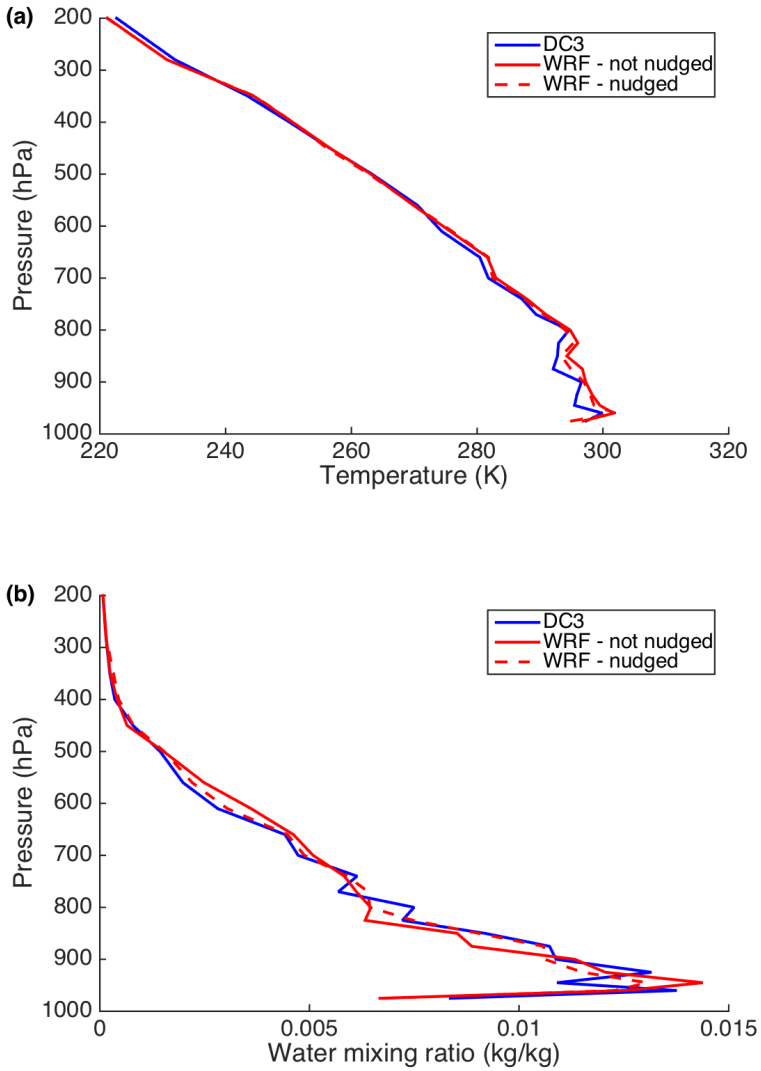

Figure S4: (a) Temperature and (b) water vapor profiles averaged over the DC3 campaign (blue) or WRF data matched to the DC3 flight path as described in Sect. 2.3 (red). WRF data resulting from the unnudged run is the solid line, data from the nudged run is the dashed line. Note that both the nudged and unnudged runs' temperature profiles agree with the DC3 profile similarly well, while the nudged water vapor profile exhibits better agreement with the DC3 profile than the unnudged one.